

LANGLEY GRANT
IN-27-CR
93165

P.75

THE EFFECTS OF MOLECULAR WEIGHT ON THE SINGLE LAP
SHEAR CREEP AND CONSTANT STRAIN RATE BEHAVIOR OF
THERMOPLASTIC POLYIMIDESULFONE ADHESIVE

Stanley K. Dembosky and Erol Sancaktar

CLARKSON UNIVERSITY

Potsdam, New York 13676

Grant NAG-1-284

February 1985

(NASA-CR-181243) THE EFFECTS OF MOLECULAR
WEIGHT ON THE SINGLE LAP SHEAR CREEP AND
CONSTANT STRAIN RATE BEHAVIOR OF
THERMOPLASTIC POLYIMIDESULFONE ADHESIVE
(Clarkson Univ.) 75 p Avail: DTIS HC

N87-27795

Unclassified
G3/27 0093165

NOMENCLATURE

\bar{M}_n	number average molecular weight
\bar{M}_w	weight average molecular weight
$\gamma, \dot{\gamma}$	one dimensional shear strain and shear strain rate
$\tau, \dot{\tau}$	one dimensional shear stress and shear stress rate
τ_y	elastic limit (yield) shear stress
γ_y	elastic limit (yield) shear strain
G_0, G	elastic shear modulus
G_1	viscoelastic shear modulus
η	viscosity coefficient
K, n	material constants for viscosity equation
D, m, a, b, r, d	material constants for nonlinear equations
τ_{ult}	ultimate shear stress
θ	elastic limit shear stress
ϕ	elastic limit shear strain
k, n	material constants
σ	plane stress
ϵ	plane strain
X, K	time dependent material properties
A', B', C'	material constants of Crochet's equation
A, B, C	material constants of Crochet's equation in shear and of creep relations based on Crochet's equation in shear
τ_0	level of constant stress
$Y(t)$	time dependent stress

LIST OF FIGURES

Figure		Page
1	The Viscoelastic Chase-Goldsmith Model Used to Describe Adhesive Behavior.	10
2	Clip-on Gage Attachment to the Single Lap Specimen for Adhesive Deformation Measurement.	26
3	Constant Strain Rate Stress Strain Behavior of Thermoplastic Polyimidesulfone Adhesive and Comparison with Theory.	28
4	Variation of Elastic Shear Modulus with Molecular Weight for Thermoplastic Polyimidesulfone Adhesive.	30
5	Variation of Viscosity with Molecular Weight for Thermoplastic Polyimidesulfone Adhesive.	32
6	Constant Strain Rate Stress Strain Behavior of Thermoplastic Polyimidesulfone Adhesive and Comparison with Theory.	33
7	Constant Strain Rate Stress Strain Behavior of Thermoplastic Polyimidesulfone Adhesive and Comparison with Theory.	35
8	Variation of Ultimate Shear Stress with Molecular Weight for Thermoplastic Polyimidesulfone Adhesive.	38
9	Variation of Maximum Shear Stress with Initial Elastic Strain Rate for Different End-Cap Forms of Thermoplastic Polyimidesulfone Adhesive.	39
10	Variation of Maximum Shear Strain with Initial Elastic Strain Rate for Different End-Cap Forms of Thermoplastic Polyimidesulfone Adhesive.	40
11	Constant Strain Rate Stress Strain Behavior of Thermoplastic Polyimidesulfone Adhesive and Comparison with Theory.	42
12	Constant Strain Rate Stress Strain Behavior	

	of Thermoplastic Polyimidesulfone Adhesive and Comparison with Theory.	43
13	Constant Strain Rate Stress Strain Behavior of Thermoplastic Polyimidesulfone Adhesive and Comparison with Theory.	44
14	Creep Behavior of Three Percent End-Cap Thermoplastic Polyimidesulfone Adhesive at 70°F (21°C) Condition.	48
15	Creep Behavior of Three Percent End-Cap Thermoplastic Polyimidesulfone Adhesive at 250°F (121°C) Condition.	49
16	Creep Behavior of Three Percent End-Cap Thermoplastic Polyimidesulfone Adhesive at 350°F (177°C) Condition.	50
17	Creep Behavior of One Percent End-Cap Thermoplastic Polyimidesulfone Adhesive at 70°F (21°C) Condition.	51
18	Creep Behavior of One Percent End-Cap Thermoplastic Polyimidesulfone Adhesive at 250°F (121°C) Condition.	52
19	Creep Behavior of One Percent End-Cap Thermoplastic Polyimidesulfone Adhesive at 350°F (177°C) Condition.	53
20	Variation of Creep Strains at 50 Minutes with Molecular Weight for Thermoplastic Polyimidesulfone Adhesive.	54
21	Creep Rupture Data and Comparison with Theory for Three Percent End-Cap Thermoplastic Polyimidesulfone Adhesive.	58
22	Creep Rupture Data and Comparison with Theory for One Percent End-Cap Thermoplastic Polyimidesulfone Adhesive.	59
23	Creep Rupture Data and Comparison with Theory for Zero Percent End-Cap Thermoplastic Polyimidesulfone Adhesive.	60
24	Variation of Maximum (Safe) Creep Stress with Molecular Weight for Thermoplastic Polyimidesulfone Adhesive.	61

25

Variation of Maximum (Safe) Creep Stress
with Environmental Temperature for Different
End-Cap Forms of Thermoplastic Polyimidesul-
fone Adhesive.

62

ABSTRACT

The bonded shear creep and constant strain rate behaviors of zero, one, and three percent endcapped Thermoplastic Polyimidesulfone adhesive were examined at room and elevated temperatures. Endcapping was accomplished by the addition of phthalic anhydrides. Single lap specimens with titanium adherends were provided by NASA-Langley Research Center. Mechanical testing was performed at Clarkson University.

The primary objective was to determine the effects of molecular weight on the mechanical properties of the adhesive. Viscoelastic and nonlinear elastic constitutive equations were utilized to model the adhesive. Ludwik's and Crochet's relations were used to describe the experimental failure data. The effects of molecular weight changes on the above mentioned mechanical behavior were assessed.

The viscoelastic Chase-Goldsmith and elastic nonlinear relations gave a good fit to the experimental stress strain behavior. Crochet's relations based on Maxwell and Chase-Goldsmith models were fit to delayed failure data. Ludwik's equations revealed negligible rate dependence. Ultimate stress levels and the safe levels for creep stresses were found to decrease as molecular weight was reduced.

CHAPTER 1

INTRODUCTION

The characterization and optimization of adhesives is essential to the production of bonded joints which are strong and reliable. Structural adhesives are widely employed by aerospace, automotive, naval and other industries. Adhesives provide a practical means for joining lightweight materials such as composites and metals, while reducing stress concentrations and maintaining structural integrity.

The model adhesive for the present investigation, Thermoplastic Polyimidesulfone, is a novel thermoplastic adhesive currently under development at NASA-Langley Research Center. It is solvent resistant and can be used in thermal environments with temperatures up to 450 °F (232 °C) [1].

In an attempt to maximize mechanical strength and bonding properties, while reducing moisture penetration [2], NASA has provided specimens of varying molecular weight for mechanical testing at Clarkson University. Molecular weights were varied by the addition of phthalic anhydride end-caps. The degree to which changes in molecular weight affects the viscoelastic properties of Thermoplastic Polyimidesulfone will be studied at room and high

temperatures. Single lap samples (ASTM D1002 standard geometry) are used because they are common to many structural fabrications where adhesives are used.

The designer of adhesively bonded joints must take into account three possible modes of failure:

- 1) failure of the adhesive layer when the rupture stress is reached under monotonic loading;
- 2) delayed failure caused by creep under a sustained load;
- 3) adherend failure.

Adhesive failure in the creep and constant strain rate modes, the effects of molecular weight upon these modes of failure, and the adhesive's stress strain behavior in general, will be discussed in this paper. Adherend failure is not a prominent consideration for the specimens used.

Objective

The purpose of this investigation is to provide insight to the effects of molecular weight on the creep and constant strain rate behavior of Thermoplastic Polyimidesulfone. The basic objectives are to:

- obtain experimental data on the delayed failure behavior of zero, one, and three percent endcapped Thermoplastic Polyimidesulfone-titanium single lap specimens;

- obtain experimental data on the constant shear strain rate behavior of the specimens;
- determine if Crochet's equation describes the delayed failure observed;
- identify a viscoelastic or nonlinear model which will describe the mechanical behavior of the adhesive;
- determine if Ludwik's equation is applicable;
- determine the effects of molecular weight on the above mentioned mechanical properties of Thermoplastic Polyimidesulfone based on experimental data.

Literature Review

The magnitude of their molecular weights is known to affect the mechanical strength of adhesives. The effects vary from material to material, and are most evident in the cohesive (pertaining to the cohesive matrix) and adhesive (pertaining to the interface) strengths of the adhesive.

The two most commonly used expressions for molecular weight are the number average (\bar{M}_n) and, weight average (\bar{M}_w) molecular weights as defined below:

$$\bar{M}_n = \frac{\sum_i N_i M_i}{\sum_i N_i} \quad (1)$$

$$\bar{M}_w = \frac{\sum_i N_i M_i^2}{\sum_i N_i M_i} \quad (2)$$

In equations (1) and (2) N_i and M_i refer to the number of molecules and the molecular weight of each species, respectively. The number average molecular weight can be calculated from boiling point, freezing point, vapor pressure, osmotic pressure, and end-group analysis of a polymer; whereas the weight average molecular weight is found by diffusion, light scattering, or ultracentrifugation [3]. Although many authors fail to state which molecular weight relation is being used, Alfrey suggests that the use

of the number average molecular weight is more useful from the concept of polymer strengths. The number average gives preferential weighting to the effects of low molecular weight segments (even a small fraction of low molecular weight material represents a large number of molecules) [4].

Very little research has been performed on the effects of molecular weight on adhesives in the bonded form, where joint failures may occur at the adhesive-adherend interface. Tsuji, Masuoka and Nakao studied the effects of molecular weight on the peel strength of polyisobutylene used to bond polyethylene films [5]. Their results show increasing peel strength with increasing molecular weight up to a maximum value. Then, with further increases in molecular weight, the peel strength decreases abruptly due to adhesive/adherend interfacial failure. This behavior is attributed to reduced wetting and adhesive behavior of the polymer at increased molecular weight values.

When an adhesive joint fails within the adhesive, and not at the adhesive-adherend interface, the mode of failure is cohesive. Zhurkov presented a theory stating creep rupture failures in the cohesive mode to be dependent on the rupture of chemical bonds within the polymer [6]. Increasing creep strength will result from increasing molecular weight because a material of higher molecular weight yields more chemical bonds. Zhurkov's experiments on

Nylon 6 fibres supported his theory. The limitation of Zhurkov's theory was the conditions under which he performed the experiments. The Nylon 6 fibres used were highly oriented. Orientation increases the intermolecular forces between the monomeric segments of neighboring molecules, and even though the intermolecular forces are much weaker than the primary valence forces within a chain, addition of intermolecular forces can become great enough to cause rupture to occur within the chains [4]. This tends to decrease the chances of failure due to stress concentrations, chain ends, chain slippage, and other factors which may be affected by changes in molecular weight and molecular weight distribution. In crosslinked and network structures with chain entanglements (usually common to structural adhesives), the polymer will not have a high degree of orientation, permitting fracture to initiate at other points besides the chemical bonds.

Because of the finite length of the polymer chains and imperfections in network geometry, initial breaking of intermolecular bonds is most likely until the stress can be carried by the remaining chain structure which is strong enough to carry the applied stress [7]. The force applied to a bulk adhesive must be perceived first by the intermolecular bonds. The disintegration of these bonds will largely determine the strength of the adhesive. Therefore, an adhesive with lower molecular weight will

reach a level of catastrophic failure at lower stress levels due to the decreased number of intermolecular bonds.

It is possible that an optimum molecular weight can be reached for an adhesive. Margolies [8] suggests that increasing molecular weight beyond an optimum value increases chain entanglement to the point where chain straightening under an applied stress is greatly inhibited. This results in chemical bond failure with the possibility that the strength of many of the polymer chains is not being utilized. Decreasing the molecular weight below the optimum point may lead to failure by chain slippage. In this case a chain orientation which is prone to slippage will be achieved more rapidly because of decreased viscosity and lower intermolecular forces.

Fellers and Kee [9] report that the number average molecular weight of polystyrene must be greater than $2M_e$ for the material to be useful. M_e is stated to be the chain entanglement molecular weight. At molecular weights below $2M_e$ the network of entangled chains is insufficient to sustain plastic flow before failure. This leads to low tensile strength and brittle fracture. Above $2M_e$ the polystyrene shows increasing rupture elongation and tensile stress with increasing molecular weight.

Although molecular rupture has been interpreted as being a process of flow, reorientation, or bond rupture, these phenomena are not clearly separated [10]. Without

specific regard to the microscopic behavior of a material, Alfrey [4] offers the opinion that the dependence of mechanical strength of a high polymer upon molecular weight is qualitatively the same for all polymers. Tensile strength is proportional to molecular weight, increasing as molecular weight increases, up to a limiting value. Once a certain molecular weight is reached, further increase in molecular weight does not result in appreciable improvements in strength. Alfrey states that low molecular weight polymers break mainly by pulling apart entangled chains, while high molecular weight specimens fail largely by the rupture of primary valence chains.

Gardner and Martin [11] observed behavior similar to Alfrey's qualitative explanation. Lexan 141 samples were subjected to molecular weight reductions by humid aging, and then tested in tension. Humid aging reduced the molecular weight by partial disintegration of the polymer chains. The results indicate a critical molecular weight value, below which, tensile strength dropped off rapidly with decreases in molecular weight. Above the critical molecular weight the tensile strength showed little increase with molecular weight. The results of the study also revealed a transition from ductile to brittle failure as the molecular weight was decreased. This was attributed to the effects of annealing caused by the aging process used. The elongation also decreased rapidly as the molecular weight decreased, and no

indication was given that the elongation will reach a plateau at higher molecular weights.

Vlachopoulos [12] reports an increase in rupture elongation with increasing molecular weight. Experiments with monodisperse ($\bar{M}_n = \bar{M}_w$) polystyrene exhibited increasing tensile strength and increasing rupture elongation as molecular weight was increased. Shinozaki [13] found similar results with his studies on PVC.

Schenck [14] investigated the mechanical behavior of zero percent endcapped thermoplastic polyimidesulfone at four temperature levels. His results provide a set of data to be used in conjunction with the present investigation.

CHAPTER 2

ANALYTICAL CONSIDERATIONS

A convenient way of relating the mechanical properties of a viscoelastic material to its molecular weight is through viscosity. The viscosity coefficient in a viscoelastic model represents a dashpot within the schematic of the model, signifying some degree of fluid-like behavior. The Chase-Goldsmith model (which is a modified form of the three parameter solid model) incorporates viscosity into material characterization in this manner (see figure 1). A sliding element prevents the dashpot from affecting the stress strain behavior until after an initial linear elastic response is seen.

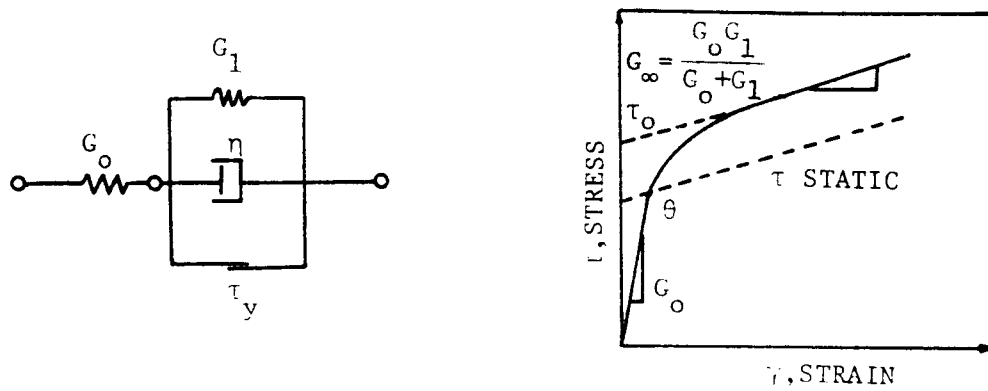


Figure 1. The Viscoelastic Chase-Goldsmith Model
Used to Describe Adhesive Behavior

A similar behavior was observed during our experiments with Thermoplastic Polyimidesulfone adhesive. This behavior was also similar to that of another polyimide adhesive (LARC-3) which was characterized previously at Clarkson. Sancaktar and Padgilwar sucessfully used the Chase-Goldsmith model to characterize the constant strain rate behavior of LARC-3 adhesive [15].

In shear, the constitutive equations for the Chase-Goldsmith model are:

$$\dot{\gamma} = \frac{\dot{\tau}}{G_0} , (\tau \leq \tau_s)$$

$$\dot{\gamma} = \frac{\dot{\tau}}{G_0} + \frac{1}{\eta} (\tau - \tau_s), (\tau > \tau_s) \quad (3)$$

where

$$\tau_s = \frac{G_0}{G_0 + G_1} (\tau_y + G_1 \gamma) \quad (4)$$

and

$$\eta = \frac{G_0}{G_0 + G_1} \eta \quad (5)$$

The constants appearing in the Chase-Goldsmith model, τ , τ_y , γ , γ_y , G_0 , G_1 , and η , represent the shear stress, yield stress, shear strain, shear strain at the yield stress, initial elastic shear modulus, the

viscoelastic shear modulus, and the viscosity coefficient, respectively.

To obtain the constant strain rate relation, the above constitutive equation is solved according to the condition

$$\dot{\gamma} = R = \text{constant} \quad (6)$$

to result in

$$\begin{aligned} \tau &= \frac{G_0}{G_0 + G_1} \{ (\tau_y + \eta R + G_1 \gamma) (1 - \exp[-\alpha(\gamma - \gamma_y)]) \} \\ &+ \{ \tau_y + \frac{G_1 G_0}{G_0 + G_1} (\gamma - \gamma_y) \} \exp[-\alpha(\gamma - \gamma_y)] \end{aligned} \quad (7)$$

where

$$\gamma_y = \frac{\tau_y}{G_0} \quad (8)$$

and

$$\alpha = \frac{G_0}{\eta R} \quad (9)$$

The material constants, including the viscosity coefficient, η , appearing in equation (7) can be evaluated from constant strain rate data. The coefficient of viscosity is a function of a number of environmental parameters such as temperature and rate, and process variables such as the polymeric molecular weight. Nielsen [16] suggests the use of equation

$$\log \eta = \log K + n \log M \quad (10)$$

where n is equal to 3.4

for relating the viscosity coefficient to the molecular weight M . This relation was derived empirically by Fox and Flory [17] based on viscosity-temperature experiments with polyisobutylene fractions. The constant K of equation (10) is dependent on the solvent and temperature, and n was found to be equal to 3.4 for polyisobutylene samples with number average molecular weights above 17,000. Nielsen suggests that equation (10) is valid for polymeric materials having molecular weights above the critical molecular weight. The critical molecular weight is defined as the value above which the polymer chains become long enough for chain entanglements to form [9]. Apparently sufficient information on the chemical structure of a material is necessary to evaluate the constant K .

Comparison between the constant strain rate data of Thermoplastic Polyimidesulfone and the behavior predicted through application of the Chase-Goldsmith model are presented in Chapter 4. A comparison between the viscosities used to fit the Chase-Goldsmith model and those predicted by equation (10) can also be found in Chapter 4.

It should be pointed out that equation (10) does not account for any variation in adhesion at the adhesive-adherend interface. Increasing viscosity tends to hinder wetting and diffusion at the interface during bond

formation [18]. This can result in inferior bonds at higher molecular weights. Observations of the fracture surfaces of one and three percent endcapped Thermoplastic Polyimidesulfone specimens reveal the presence of such behavior.

When the effects of rate on stress strain behavior are not strong, the use of a nonlinear elastic-plastic model may be adequate. One such model is the Ramberg-Osgood model which is based on Hencky's stress strain relations [19]. This theory assumes the plastic strains to be functions of the current state of stress and independent of the loading history. In one dimension the Ramberg-Osgood relation has the form

$$\gamma = \frac{\tau}{G} + D \tau^m \quad (11)$$

where γ is the shear strain, τ is the shear stress, G is the elastic shear modulus, and D and m are material constants. The constant m denotes the plastic flow, and consequently the work-hardening characteristics. This model can be modified to account for rate effects. For example, Brinson and Renieri used a rate dependent version of the Ramberg-Osgood model to characterize Metlbond 1113 and 1113-2 thermosetting (epoxy) adhesives in the bulk form [19]. For the present investigation, observations revealed that separation of the linear and nonlinear terms of

equation (11) into the form

$$\gamma = \frac{\tau}{G}, \quad (\tau \leq \tau_y) \quad (12)$$

$$\gamma = D \tau^m, \quad (\tau < \tau_y) \quad (13)$$

would provide a more adequate representation of the observed stress strain behavior.

Schenck used a nonlinear equation of the form

$$\tau = a\gamma^b \quad (14)$$

where

τ = the shear stress

γ = the shear strain

and

a and b are material constants

to characterize the constant strain rate behavior of the zero percent encapped form of Thermoplastic Polyimidesulfone [14]. Apparently equation (14) is not separated into linear and nonlinear segments as in equations (12) and (13). However, results of the current investigation revealed that a more accurate representation could be derived for Thermoplastic Polyimidesulfone adhesives of different molecular weights using equations (12) and (13).

The rate dependence of the rupture stresses under constant strain rate conditions can be expressed with the semiempirical equation proposed for metals by Ludwik in the form

$$\tau_{Ult} = \tau' + \tau'' \log \left(\frac{\dot{\gamma}}{\dot{\gamma}'} \right) \quad (15)$$

where τ_{Ult} is the ultimate shear stress, $\dot{\gamma}'$ is the initial elastic shear strain rate, and τ' , τ'' , and $\dot{\gamma}'$ are material constants [20]. Brinson [21] used this equation to successfully describe the rate dependence of rupture stresses for polymeric materials in the bulk tensile mode.

The same form of equation (15) can also be used to describe the variation of shear rupture stress (θ) and strains (ϕ) with initial elastic shear strain rates in the bulk and bonded forms. These relations may be written as

$$\theta = \theta' + \theta'' \log \left(\frac{\dot{\gamma}}{\dot{\gamma}'} \right) \quad (16)$$

$$\phi = \phi' + \phi'' \log \left(\frac{\dot{\gamma}}{\dot{\gamma}'} \right) \quad (17)$$

where additional material constants are defined accordingly.

Delayed failure of an adhesive can be described with the use of Crochet's creep-rupture equation (equation 21). Crochet's equation is based on Naghdi's definition of a yield surface as a function of stress (σ_{ij}), plastic strain

(ϵ_{ij}^p) , work hardening due to path history (x_{ij}) , and the time history of loading deformation (κ_{ij}) . The functional relationship

$$f = f(\sigma_{ij}, \epsilon_{ij}^p, x_{ij}, \kappa_{ij}) = 0 \quad (18)$$

was simplified [20] with the use of a Mises yield criterion to give

$$f = \frac{1}{2} S_{ij} S_{ij} - k^2 = 0 \quad (19)$$

$$k = k(x, \kappa) \quad (20)$$

Crochet neglected the work-hardening term, on the basis of the theory of elastic perfectly plastic solids, and assumed κ to be only a function of x . Based on Crochet's assertions that κ is a monotonically decreasing function of x , and that κ has a lower bound for larger values of x , Brinson [22] mathematically interpreted the functional behavior of κ as

$$Y(t) = A' + B' \exp(-C'x) \quad (21)$$

in equation (21) $Y(t)$ is the time dependent maximum stress and A' , B' , and C' are material parameters. Crochet's specific functional form for x was

$$x = [(\varepsilon_{ij}^v - \varepsilon_{ij}^E)(\varepsilon_{ij}^v - \varepsilon_{ij}^E)]^{1/2} \quad (22)$$

where ε_{ij}^v and ε_{ij}^E refer to viscoelastic and elastic strains respectively. Sancaktar [23] interpreted equation (21) to apply to pure shear in the form

$$\tau = A + B \exp(-Cx_s) \quad (23)$$

with

$$x_s = \gamma_{12}^v - \gamma_{12}^E \quad (24)$$

where γ_{12}^v and γ_{12}^E refer to the "engineering" shear strains, and A, B, and C are material constants. Since delayed failure occurs only in elements loaded up in to the viscoelastic region, an expression for X can be obtained by subtracting the elastic shear strain from the proposed equation.

When the constant strain rate stress strain behavior of an adhesive is determined to be approximately nonlinear elastic, and the creep behavior is not characterized with a viscoelastic model, then the simplest model creep relation can be utilized for the evaluation of X. This procedure, however, should be applied only as a first approximation for practical purposes. Following the procedure for the evaluation of X in conjunction with the Maxwell model creep relation (equation 26) results in a solution to

Crochet's creep-rupture equation (equation 23) of the form

$$\tau = A + B \exp[-C\tau \frac{t}{n}] \quad (25)$$

$$\gamma = \frac{\tau_0}{n} [t + \frac{n}{G}] \quad (26)$$

A similar delayed failure equation results from the solution of equation (23) with the Chase-Goldsmith model. The resulting equation has the form

$$\begin{aligned} Y(t) = & A + B \exp \left\{ -C \left[\frac{Y}{G_1} \left(\exp \left[-\frac{G_1}{n} t \right] - 1 \right) \right. \right. \\ & + \frac{Y(t)}{G_\infty} \left(1 - \exp \left[-\frac{G_1}{n} t \right] \right) \\ & \left. \left. + \frac{Y(t)}{G_0} \left(\exp \left[-\frac{G_1}{n} t \right] - 1 \right) \right] \right\} \end{aligned} \quad (27)$$

In equation (27) the exponential terms contain viscosity coefficients as viscoelastic models are used. In this case the viscosity affects the creep rate of the material. If the material constant C of equation (27) were taken to be a constant for all degrees of endcapping, increasing the viscosity would predict a longer time to failure for a given stress level.

The asymptotic values of equations (25) and (27) represent the maximum safe creep stress levels below which

delayed failures are not expected to occur. Mathematical analysis reveals that equation (27) predicts a much faster approach to its asymptotic stress level in comparison to equation (25). These asymptotic values can be expressed as a function of temperature to represent experimental data empirically. Such application of Crochet's equation to the elevated temperature creep data is justified by the applicability of the time-temperature superposition principle to viscoelastic creep relations.

CHAPTER 3

EXPERIMENTAL PROCEDURES

Materials and Specimen Features

The preparation and bonding of Thermoplastic Polyimidesulfone has been described in detail by St. Clair [1,2]. A polyimide acid solution is formed by mixing 0.0569 lbs (25.8 gms) of 3,3',4,4'-Benzophenonetetracarboxylic dianhydride (BTDA) in a solution made of 0.0439 lbs (19.9 gms) of 3,3'-diaminodiphenylsulfone (3,3'-DDS) and 0.5701 lbs (258.6 gms) of bis (2-methoxyethyl) ether. Endcapping is accomplished through the addition of a phthalic anhydride in concentrations varying from zero to three percent. The acid solution is then brushed onto 112-E-A100 glass carrier cloth. The cloth acts as a control for bondline thickness and as a carrier for the adhesive. The scrim is then heated to 212 °F (100 °C) for one half hour, 302 °F (150 °C) for one half hour, and to 392 °F (200 °C) for one half hour. This heating process removes the solvent and the water from the adhesive.

Titanium (6-AL,4-V) strips are grit blasted with 120 mesh aluminum oxide and treated with Pasa Jell 107. A primer coating of the polyimide acid is brushed onto titanium and heated to 212 °F (100 °C) for one hour and 392 °F (200 °C) for one hour. Lap shear specimens are then formed by sandwiching the scrim between the titanium

adherends using a 0.5 inch (1.27 cm) overlap. The specimens are heated at 41 °F/min (5 °C/min) to 392 °F (200 °C); a 200 psi (1.38 MPa) clamping force is applied at this point. The specimens are then heated further to 635 °F (335 °C), held for 5 minutes, then allowed to cool to 302 °F (150 °C) before removing the bonding clamps.

All test specimens were prepared at NASA - Langley Research Center, and are in accordance with ASTM D1002 specifications.

Molecular weights were determined by membrane osmometry on a Knauer osmometer at Arro Laboratories, Ill. Information on molecular weight distribution and number average molecular weight values could not be obtained because of the cloudiness of the material. The molecular weight values reported by NASA are shown in table (1).

Table 1. Molecular Weight Values of Zero, One, and Three Percent Endcapped Thermoplastic Polyimidesulfone Adhesive.

Percent End-Cap	Molecular Weight (amu)
0.0	19700
1.0	18800
3.0	17400

The bondline thicknesses were measured using a

microscope with 40X magnification. Twenty five measurements were taken along each outside edge of the bonds. The bondline length, adherend width, and adherend thicknesses were measured with a Kanson dial caliper. Specimen dimensions are listed in tables (A-1 and A-2) in Appendix (A).

The dimensions for each specimen were needed to calculate the adhesive shear stresses and strains. The shear stress was assumed to be uniform and was calculated by dividing the applied load by the overlap area. The shear strain was calculated by the bondline elongation divided by the average bondline thickness.

Testing Methods

The mechanical testing of the single lap Polyimidesulfone samples was performed at Clarkson University. NASA - Langley Research Center supplied twenty of each one and three percent endcapped specimens. Testing on zero percent endcapped specimens was previously performed at Clarkson University by Schenck [14]. All testing was done using a Model 1331 Instron servohydraulic materials testing machine.

Each single lap specimen had notches milled 0.99 inches (2.51 cm) apart on the overlap edge of the bond. The notches were 0.01 inches (.0254 cm) deep by 0.01 inches (0.0254 cm) wide and were used for the placement of a high precision extensometer. The output signal from the extensometer was amplified through the Instron's internal amplification system. The signals from the extensometer and the load cell were then recorded on a three channel strip chart recorder. The extensometer was calibrated using a high magnification extensometer calibrator.

Output from the extensometer was used to calculate the strain in the adhesive joint. Deformations in the adherends were subtracted from the total deformation values to obtain adhesive deformations. The adherend deformations were calculated using equation:

$$\text{Adherend Deformation} = \frac{[F(D - 0)]}{[E(AT)W]} \quad (28)$$

where

F = load applied to the adherends

D = the distance between the milled notches in the
adherends of the single lap specimens, 0.99 inches
(2.51 cm)

O = overlap length

E = Young's Modulus for titanium, 15,000,000 psi
(103,421 MPa)

AT = adherend thickness, 0.05 inches (0.127 cm)

W = adherend width over the overlap area.

Creep and constant strain rate tests were performed at temperatures of 70 °F (21 °C), 250 °F (121 °C), and 350 °F (177 °C). High temperature testing was performed with an environmental chamber mounted on the testing frame of the Instron. Room temperature constant strain rate tests were conducted with crosshead rates of 0.001, 0.1, and 10.0 inches/minute (0.00254, 0.254, 25.4 cm/min). High temperature constant strain rate tests were ran at a crosshead rate of 5.0 inches/minute (12.7 cm/minute). Three to five specimens of each percent encapping were tested in creep at each temperature level. The creep tests had an initial crosshead rate of 0.3 inches/minute (0.762 cm/minute), and were performed at stress levels above the elastic limit stress found from the constant strain rate tests.

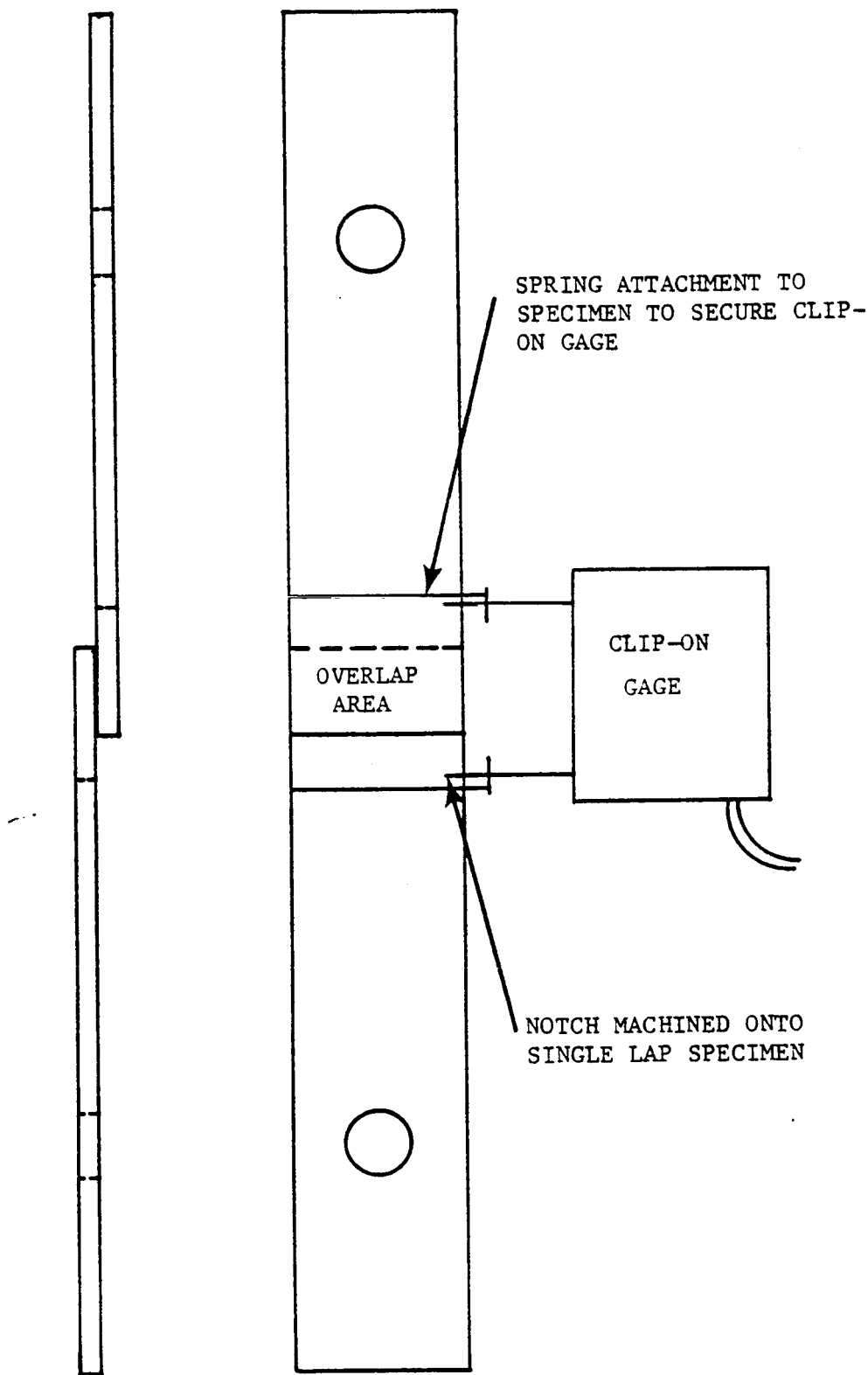


Figure 2. Clip-on Gage Attachment to the Single Lap Specimen for Adhesive Deformation Measurement.

CHAPTER 4

RESULTS AND DISCUSSION

The constant strain rate behavior of zero, one, and three percent endcapped Thermoplastic Polyimidesulfone adhesive at room temperature is shown in figure 3. The experiments displayed are all at comparable initial elastic strain rates. Experiments at 100 and 10,000 times slower rates did not exhibit strong rate dependence based on ultimate stresses and strains. The observed regions of linear elastic behavior followed by regions of visco-plastic behavior suggest that the Chase-Goldsmith model may be used to describe the constant strain rate behavior of Thermoplastic Polyimidesulfone. Behavior predicted by the Chase-Goldsmith model is also shown in figure 3. The model provides a good fit to the data at all stress levels observed. The coefficients (G_0 , G_1 , τ_y , γ^0 , and η) used to fit the model at room temperature are given in table 2.

The elastic shear modulus, G , for each endcapped form of Thermoplastic Polyimidesulfone was calculated from the experimental data by averaging the slope of the shear stress strain curve between data points in the initial linear elastic region. G was observed to increase as molecular weight increased (figure 4). The values of G_0 and G_1 used to fit the Chase-Goldsmith model at room temperature followed

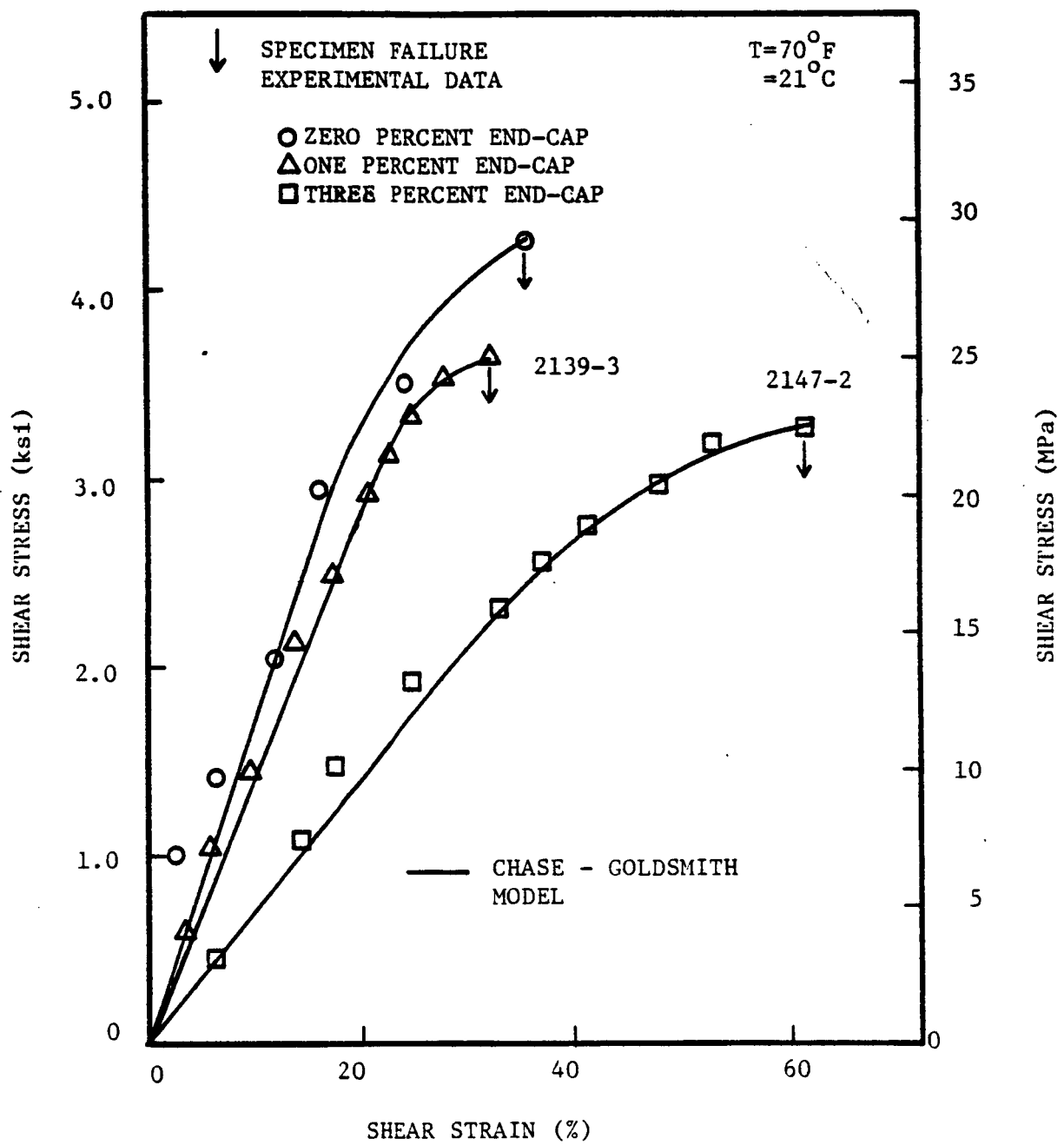


Figure 3. Constant Strain Rate Stress Strain Behavior of Thermoplastic Polyimidesulfone Adhesive and Comparison with Theory.

Table 2

Coefficients used to fit the Chase-Goldsmith model to the constant strain rate behavior of zero, one, and three percent endcapped

Thermoplastic Polimidesulfone adhesive at 70 °F (21 °C) (see figure 3)

Percent End-Cap	G_0 KSI (MPa)	G_1 KSI (MPa)	τ_y KSI (MPa)	$\dot{\gamma}_0$ %/sec	η KSI-sec (MPa-sec)
0	17.1 (117.8)	4.3 (29.6)	3.0 (20.7)	24.6	4.1 (28.2)
1	13.8 (95.1)	1.6 (11.0)	2.9 (20.0)	38.5	2.1 (14.5)
3	7.0 (48.2)	1.2 (8.3)	2.3 (15.8)	125.0	0.8 (5.5)

Chase-Goldsmith model:

$$\begin{aligned}\tau &= \frac{G}{G_0 + G_1} \{ (\tau_y + \dot{\gamma}_0 R + G_1 \gamma) (1 - \exp[-\alpha(\gamma - \gamma_y)]) \} \\ &+ \{ \tau_y + \frac{G_1 G_0}{G_0 + G_1} (\gamma - \gamma_y) \} \exp[-\alpha(\gamma - \gamma_y)]\end{aligned}$$

$$\gamma_y = \frac{\tau_y}{G_0}$$

$$\alpha = \frac{G_0}{\dot{\gamma}_0 R}$$

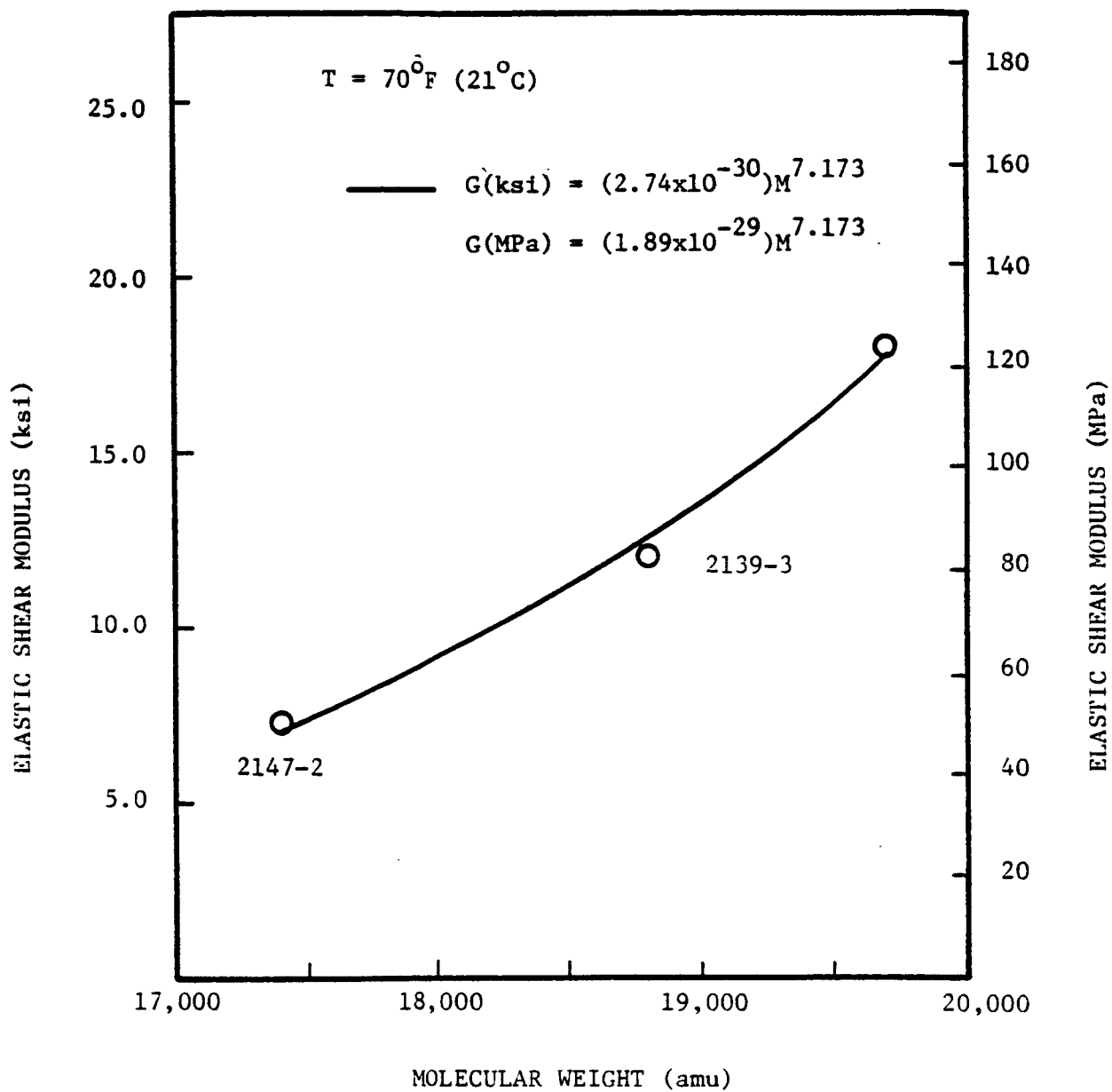


Figure 4. Variation of Elastic Shear Modulus with Molecular Weight for Thermoplastic Polimidesulfone Adhesive.

the same trend.

The viscosities found in fitting the Chase-Goldsmith model are plotted in figure 5. Equation (10) predicts a much slower increase in viscosity as molecular weight increases. The discrepancies between the two values may partially be attributed to the fact that the adhesive used for experimentation was in the bonded form rather than in the bulk form.

The constant strain rate behaviors of zero, one, and three percent endcapped Thermoplastic Polyimidesulfone at 250 °F (121 °C) and 350 °F (177 °C) are shown in figures 6 and 7 along with theoretical predictions by the Chase-Goldsmith model. The regions of linear elastic behavior followed by visco-plastic deformation are evident. It can be observed that the zero percent endcapped specimens reached higher rupture strains and lower rupture stresses in comparison to the one percent endcapped samples. This can be attributed to Schenck's [14] observation of increasing interfacial failure with increasing temperature for the zero percent endcapped specimens. This phenomena causes the coefficients of the Chase-Goldsmith model to change, thus making it impractical to compare viscosities, shear moduli, etc. for the different molecular weights at elevated temperatures. The coefficients used to fit the Chase-Goldsmith model at 250 °F (121 °C) and 350 °F (177 °C) are listed in tables 3 and 4.

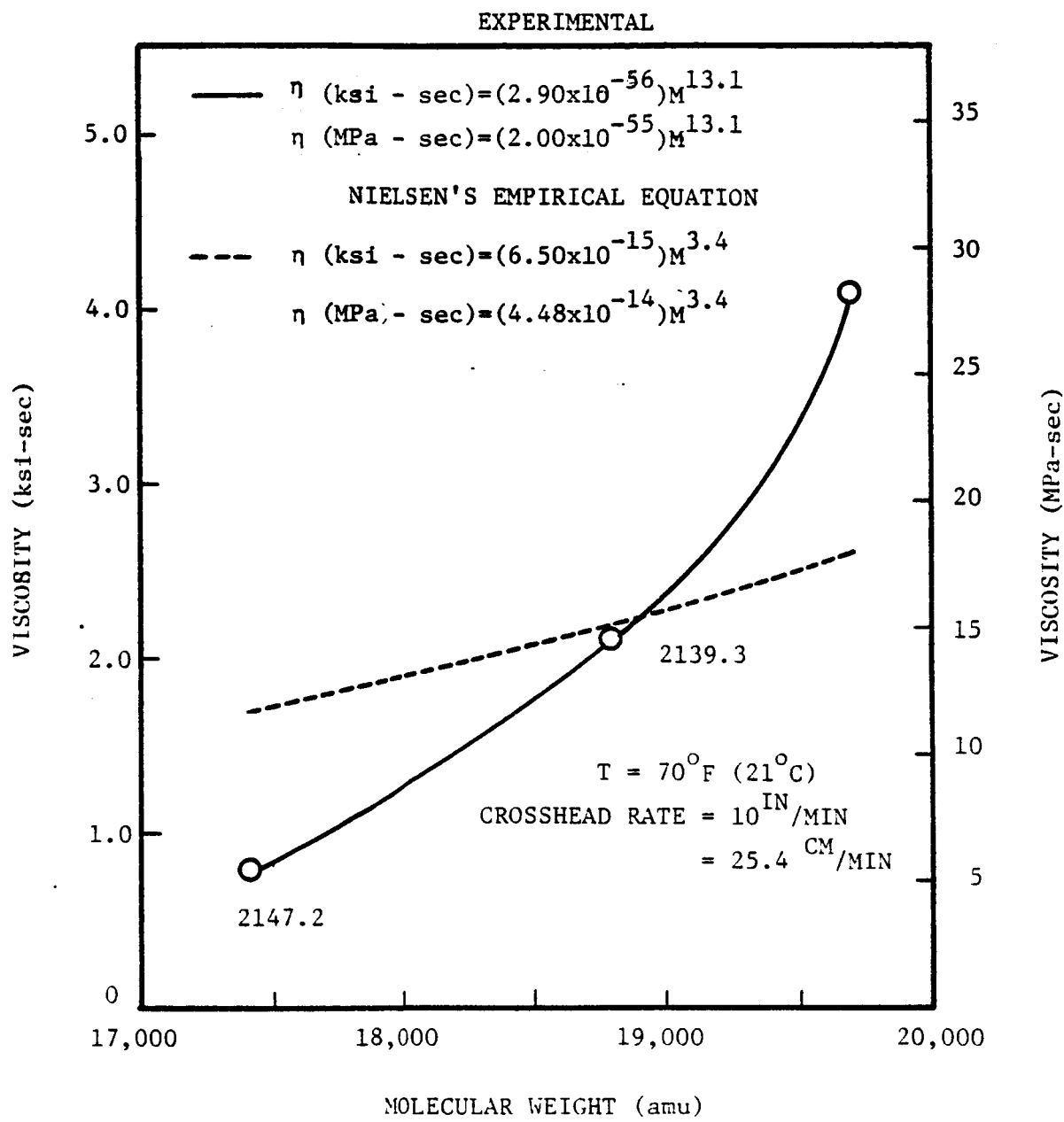


Figure 5. Variation of Viscosity with Molecular Weight for Thermoplastic Polyimidesulfone Adhesive.

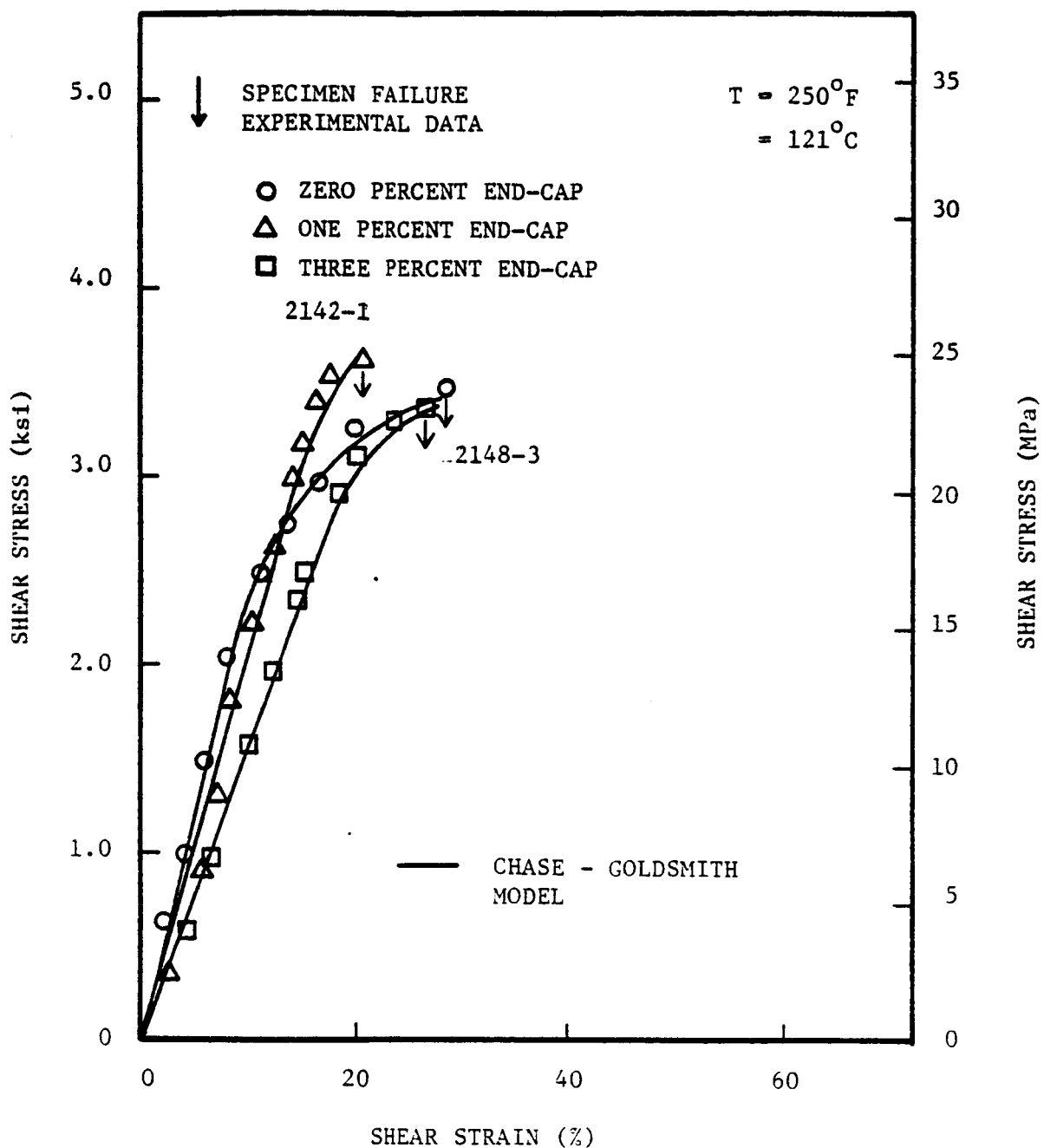


Figure 6. Constant Strain Rate Stress Strain Behavior of Thermoplastic Polyimidesulfone Adhesive and Comparison with Theory.

Table 3

Coefficients used to fit the Chase-Goldsmith model to the constant strain rate behavior of zero, one, and three percent endcapped

Thermoplastic Polimidesulfone adhesive at 250 °F (121 °C) (see figure 6)

Percent End-Cap	G_0 KSI (MPa)	G_1 KSI (MPa)	τ_y^0 KSI (MPa)	$\dot{\gamma}^0$ %/sec	η KSI-sec (MPa-sec)
0	24.2 (166.7)	2.1 (14.5)	2.3 (15.8)	59.1	1.2 (8.3)
1	20.7 (142.6)	2.2 (15.2)	3.0 (20.7)	19.4	4.0 (27.6)
3	16.5 (113.7)	2.1 (14.5)	2.7 (18.6)	20.2	2.9 (20.0)

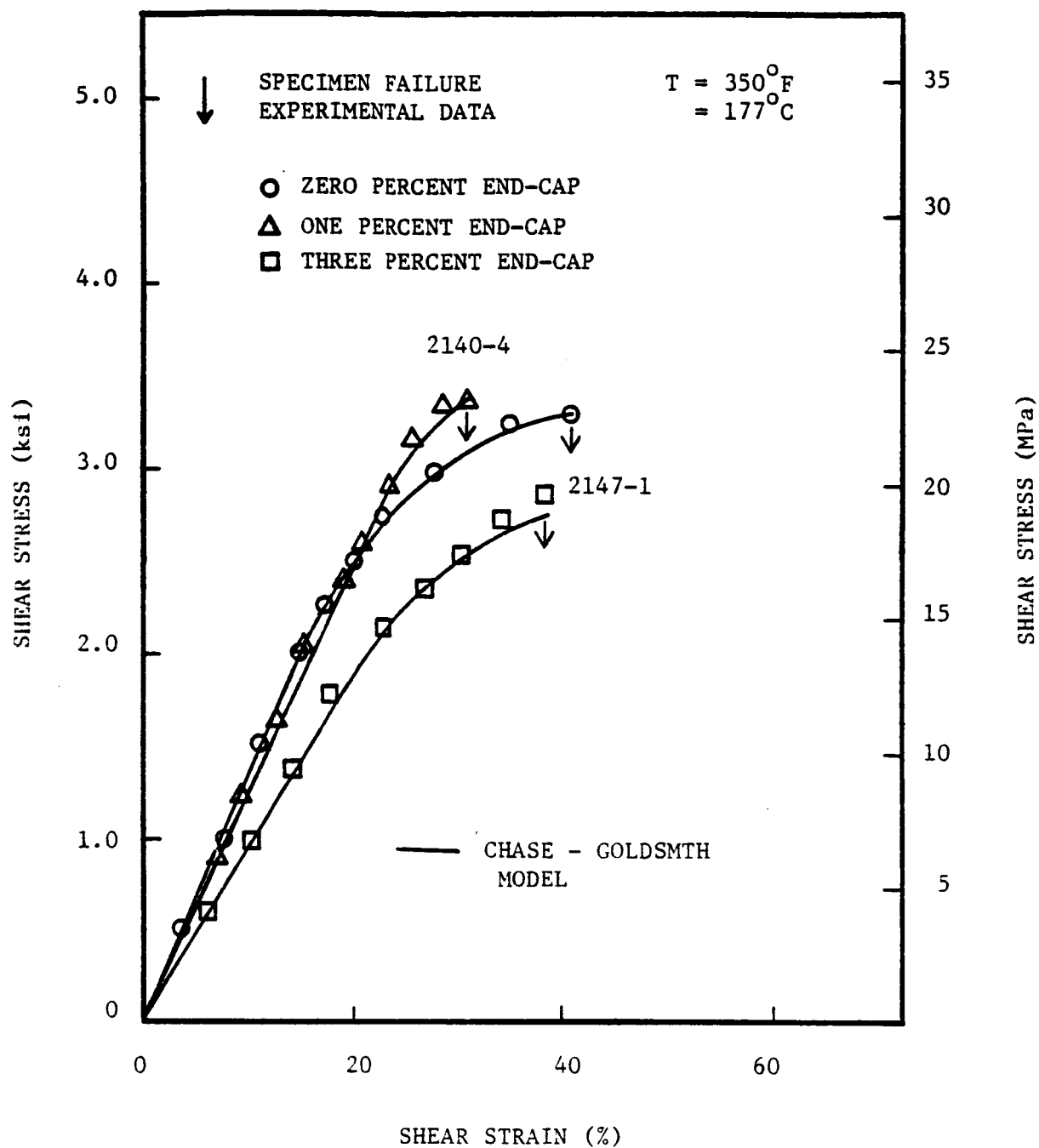


Figure 7. Constant Strain Rate Stress Strain Behavior of Thermoplastic Polyimidesulfone Adhesive and Comparison with Theory.

Table 4

Coefficients used to fit the Chase-Goldsmith model to the constant strain rate behavior of zero, one, and three percent endcapped Thermoplastic Polimidesulfone adhesive at 350 °F (177 °C) (see figure 7)

Percent End-Cap	G_0 KSI (MPa)	G_1 KSI (MPa)	τ_y^0 KSI (MPa)	$\dot{\gamma}^0$ %/sec	n KSI-sec (MPa-sec)
0	13.3 (91.6)	1.0 (6.9)	2.0 (13.8)	86.0	1.5 (10.3)
1	12.38 (84.1)	1.7 (11.7)	2.9 (20.0)	26.1	1.8 (12.4)
3	9.6 (66.1)	1.3 (9.0)	1.9 (13.1)	28.2	2.9 (20.0)

The ultimate shear stresses under constant strain rate conditions (figure 8) show the effects of the high temperature interfacial failures on the zero percent endcapped specimens. At room temperature the ultimate shear stresses increase with increasing molecular weight in a linear fashion. It should be noted that this data represent the maximum ultimate shear stress values even though other (lower) values were also obtained at different test rates. The ultimate shear stress values reported by NASA for one half and two percent endcapped Thermoplastic Polyimidesulfone specimens at room temperature also agree with the linear interpolation of increasing ultimate shear stress with increasing molecular weight. A similar linear behavior between the ultimate shear stress and molecular weight is observed at elevated temperatures. This data, however, represent results obtained using only a single crosshead rate.

Figures 9 and 10, respectively, show the variation of the ultimate shear stresses and maximum shear strains with the initial elastic shear strain rate for zero, one, and three percent endcapping. Data depicted in both figures is irregular, implying weak rate dependence which can be concealed by the effects of the fracture process and other experimental variations.

The constant strain rate behavior of Thermoplastic Polyimidesulfone can also be predicted using a nonlinear

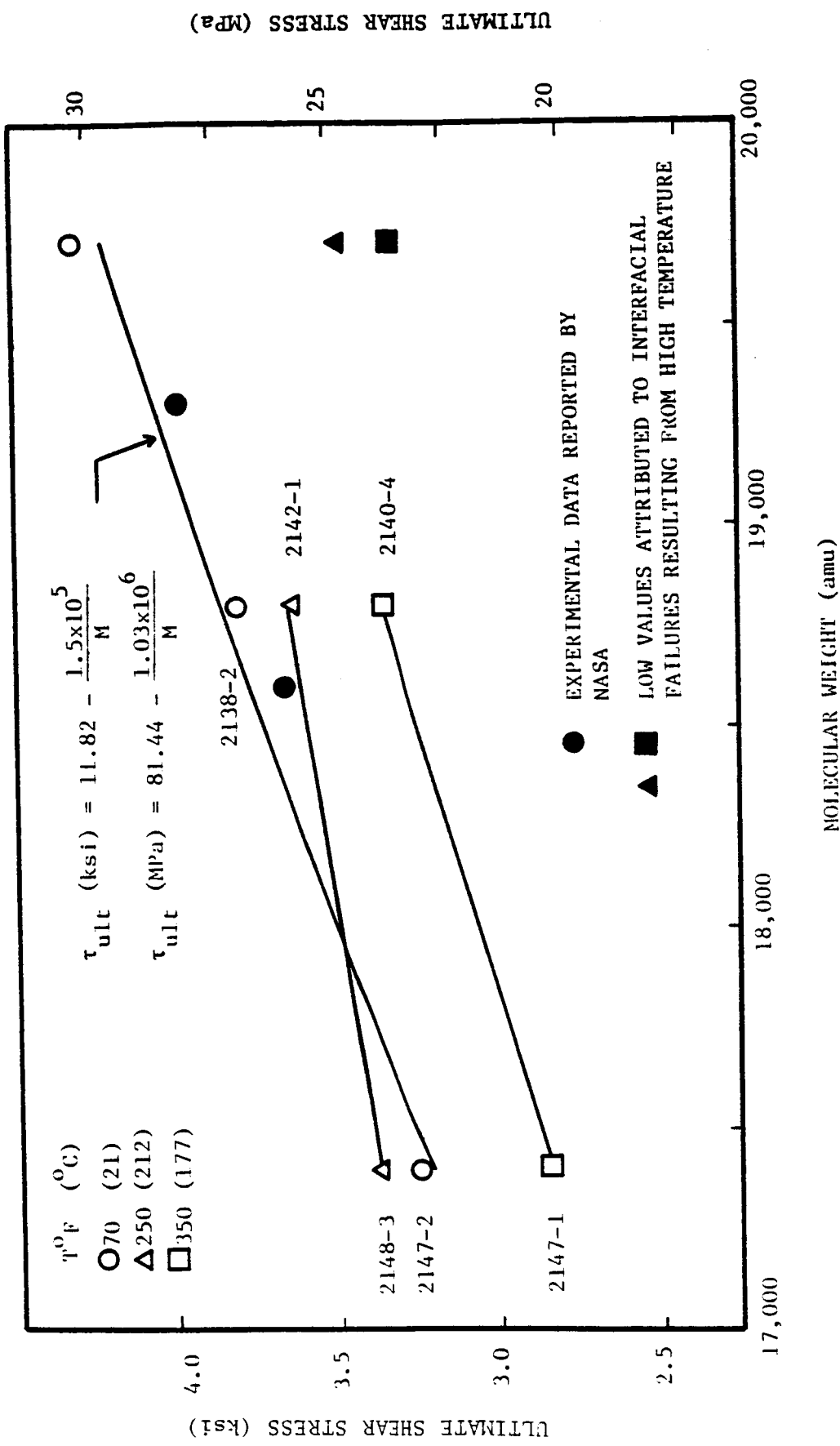


Figure 8. Variation of Ultimate Shear Stress with Molecular Weight for Thermoplastic Polyimidesulfone Adhesive.

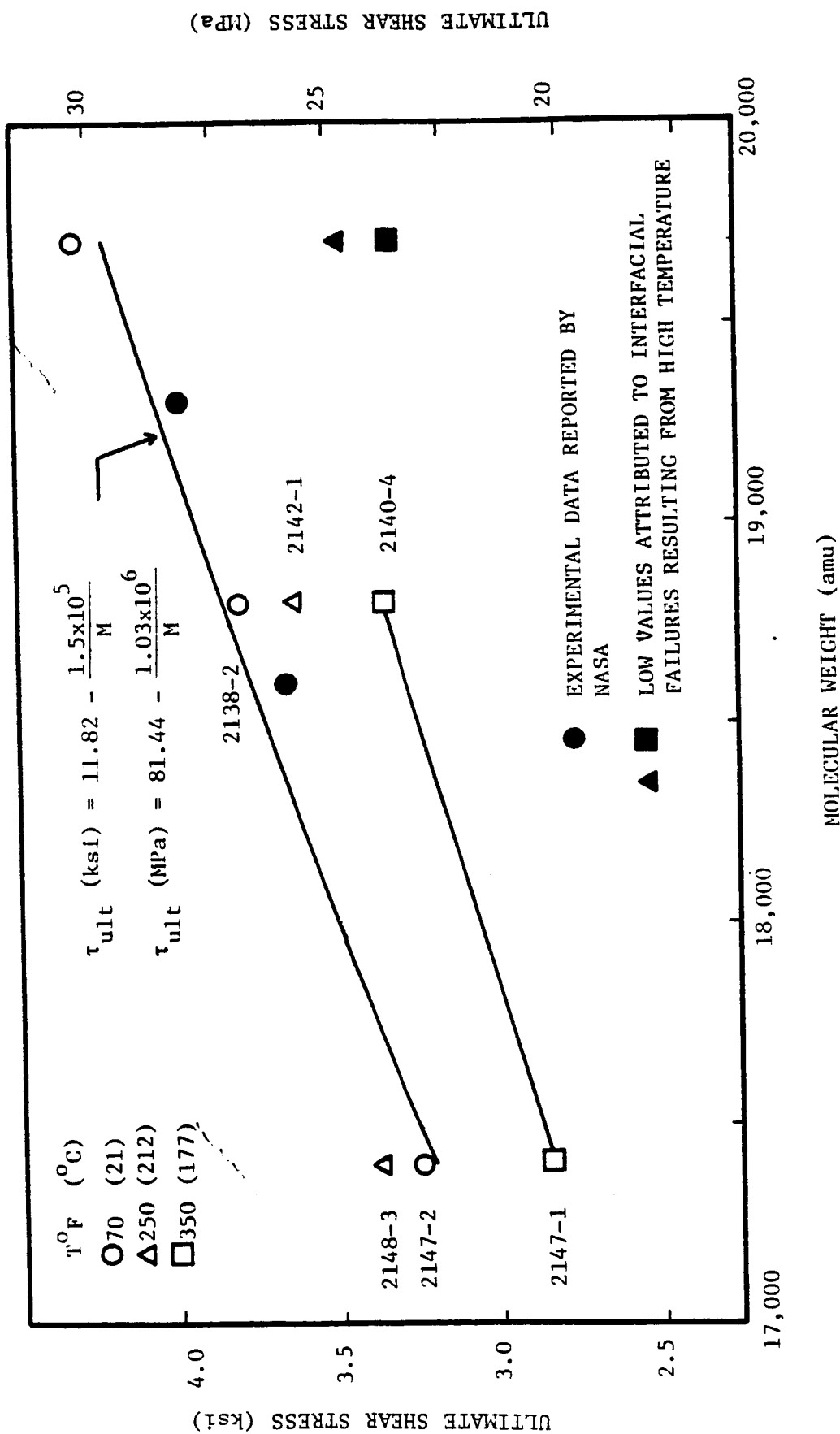


Figure 8. Variation of Ultimate Shear Stress with Molecular Weight for Thermoplastic Polyimidesulfone Adhesive.

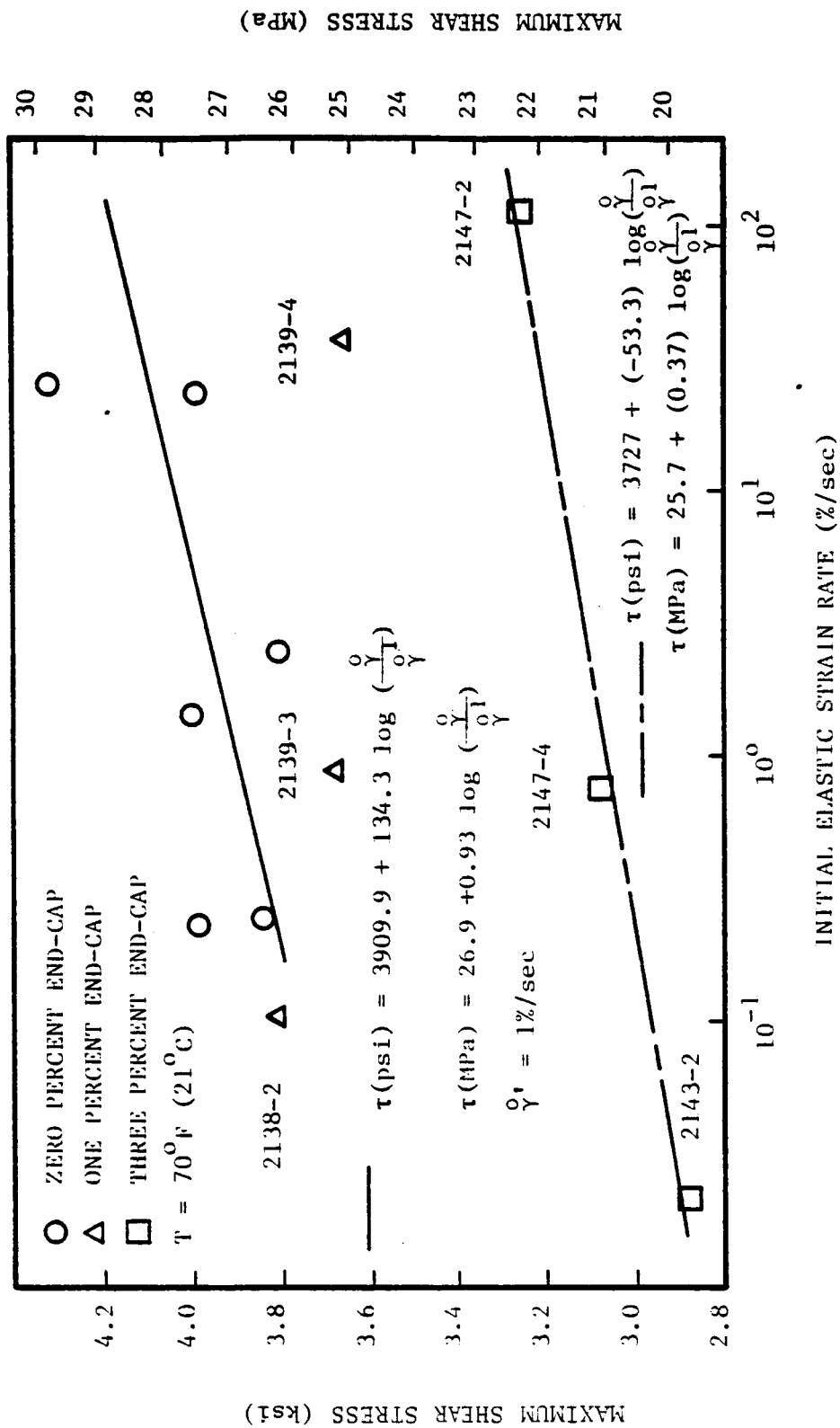


Figure 9. Variation of Maximum Shear Stress with Initial Elastic Strain Rate for Different End-Cap Forms of Thermoplastic Polyimidesulfone Adhesive.

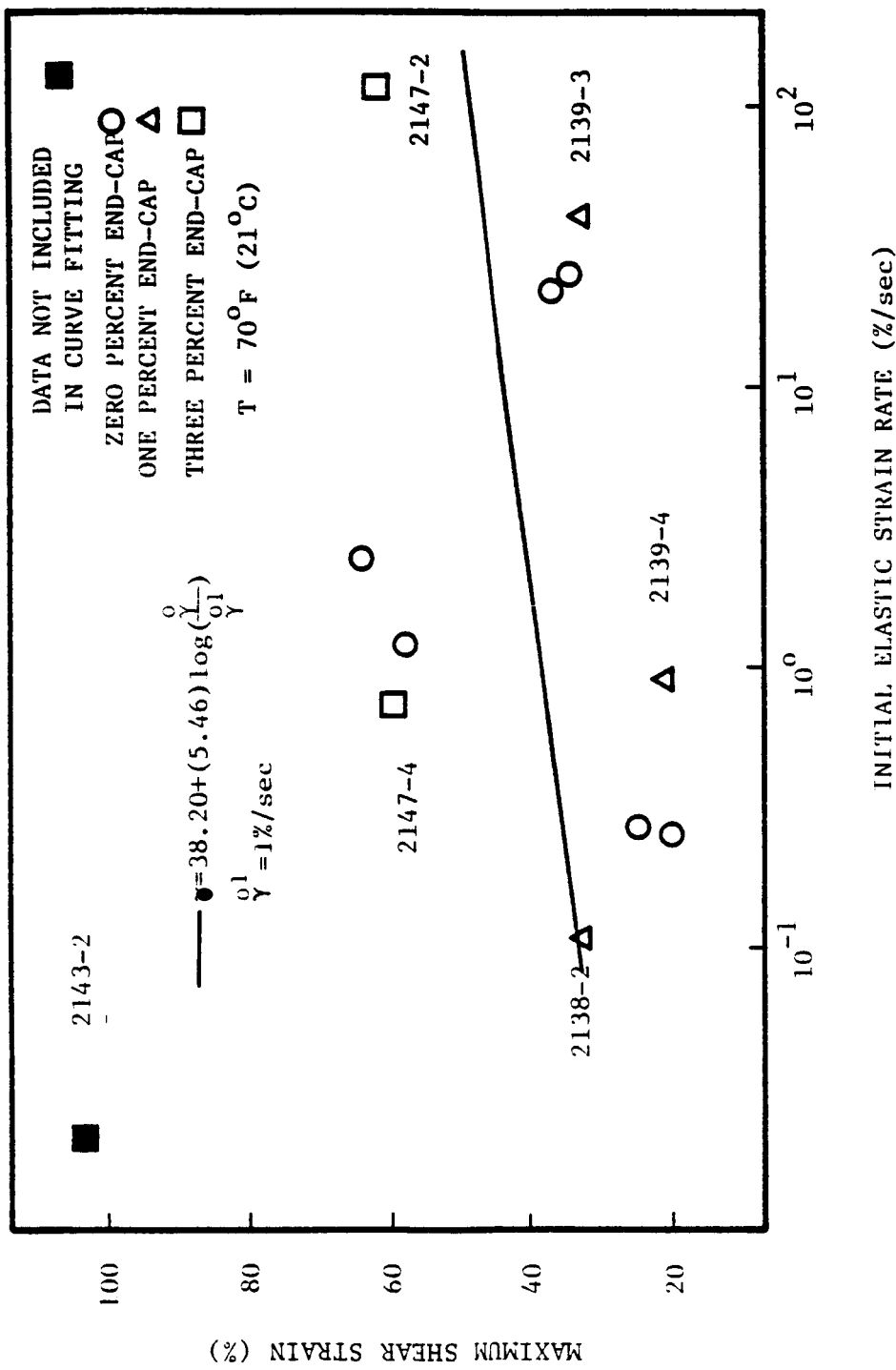


Figure 10. Variation of Maximum Shear Strain with Initial Elastic Strain Rate for Different End-Cap Forms of Thermoplastic Polyimidesulfone Adhesive

elastic approach. In figures 11, 12, and 13 it can be observed that by assuming linear elastic behavior up to the elastic limit stress, and by using a nonlinear power law equation past this limit, the constant strain rate behavior of zero, one, and three percent endcapped specimens can be predicted adequately at all temperatures tested. The coefficient, m , of the nonlinear relation used (equation 13) is determined from the experimental data. Since m is the reciprocal of the coefficient d commonly used in a power law of the form

$$\tau = r \gamma^d \quad (29)$$

it is a relative measure of the amount of work-hardening that the adhesive can withstand before failure occurs. In other words, low values of m indicate soft, ductile materials, and high values of m indicate hard brittle materials. Examination of data indicates that room temperature m decreased by 22.5 % between zero and one percent endcapping, and by 8.0 % between one and three percent endcapping. As can be seen in figure 11, toughness increases considerably when the molecular weight is increased from 17400 amu to 19700 amu. This trend was not as pronounced at elevated temperatures.

The creep results for three percent endcapped Thermoplastic Polyimidesulfone at 70 °F (21 °C), 250 °F (121

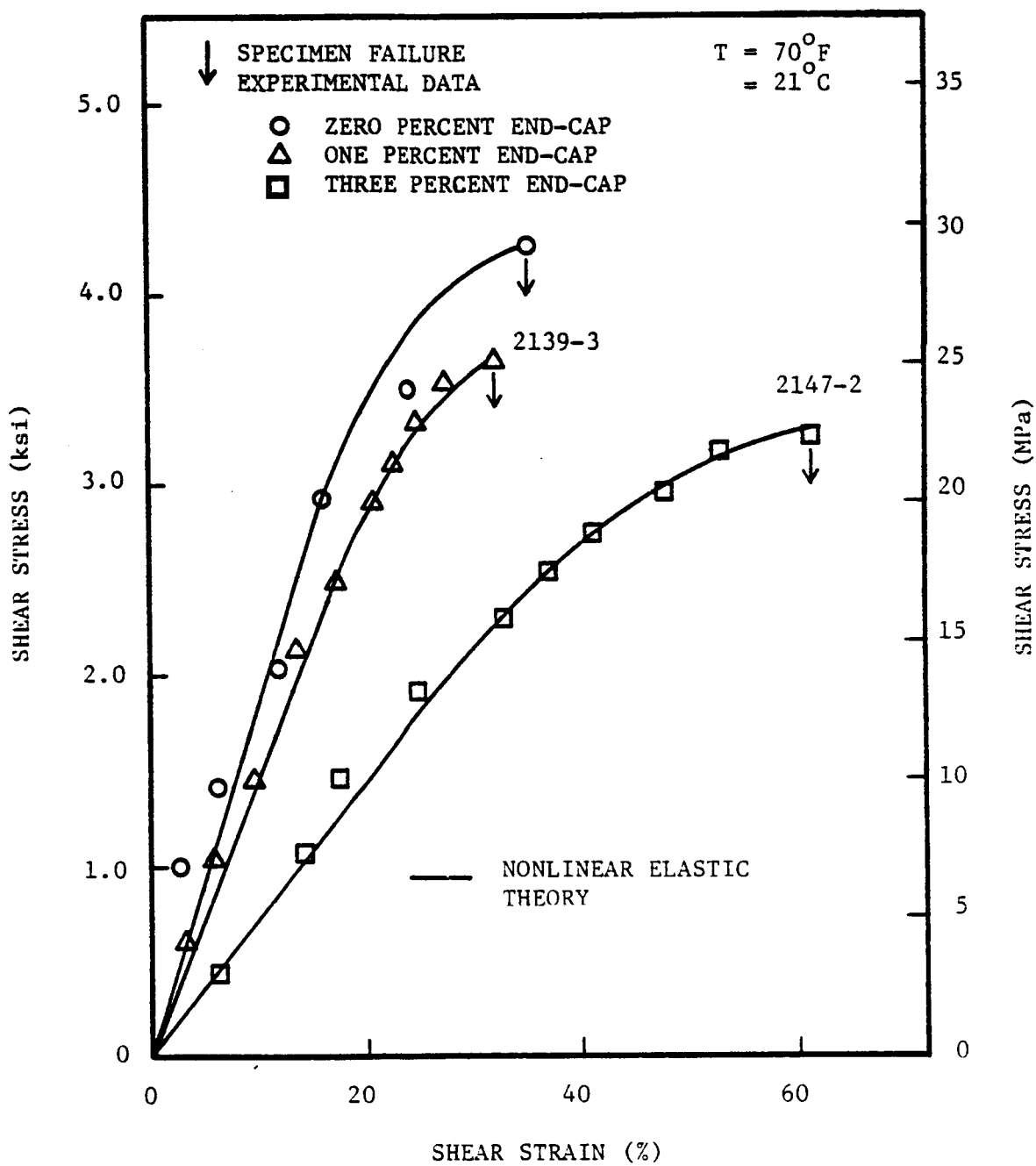


Figure 11. Constant Strain Rate Stress Strain Behavior of Thermoplastic Polyimidesulfone Adhesive and Comparison with Theory.

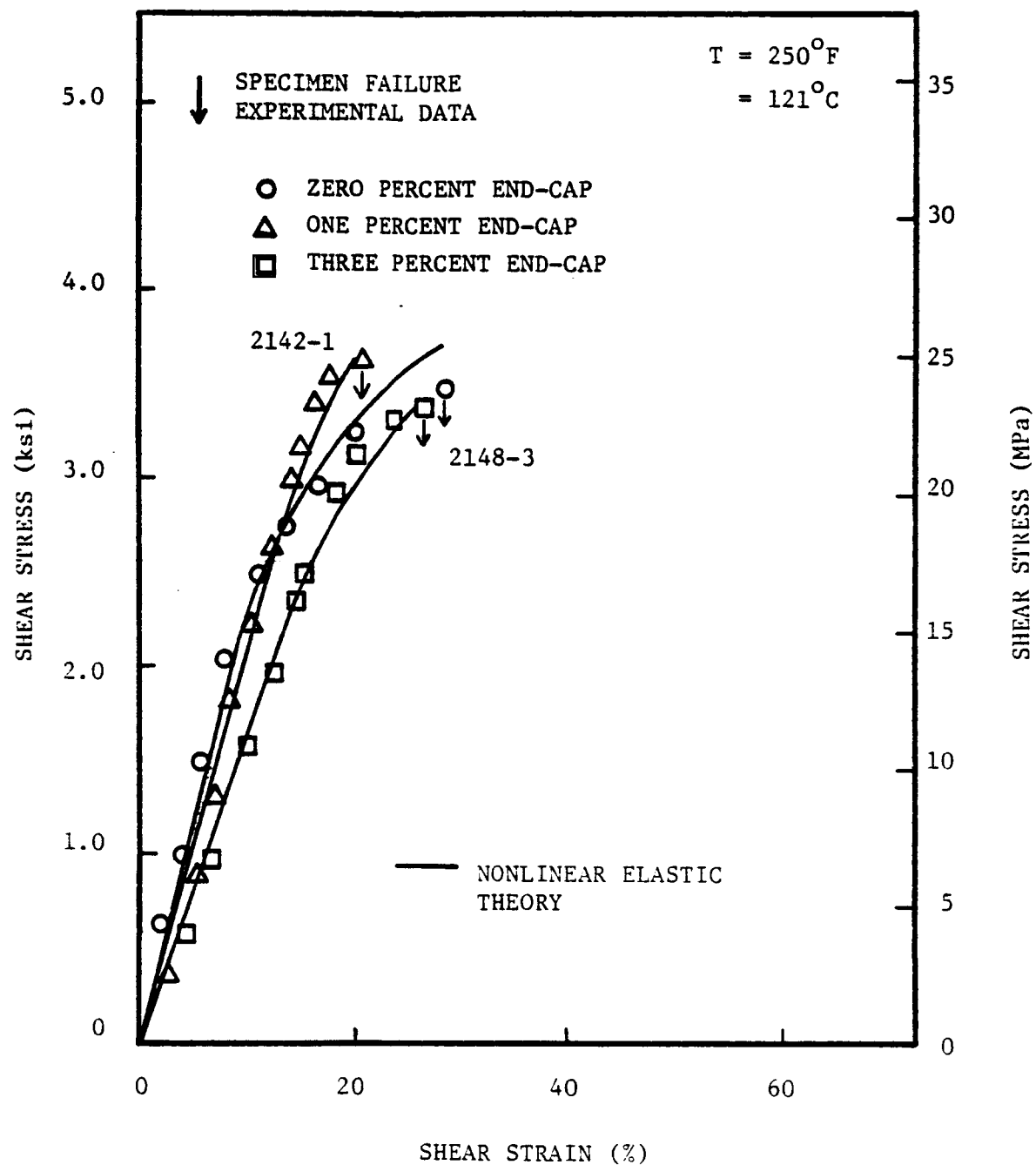


Figure 12. Constant Strain Rate Stress Strain Behavior of Thermoplastic Polyimidesulfone Adhesive and Comparison with Theory.

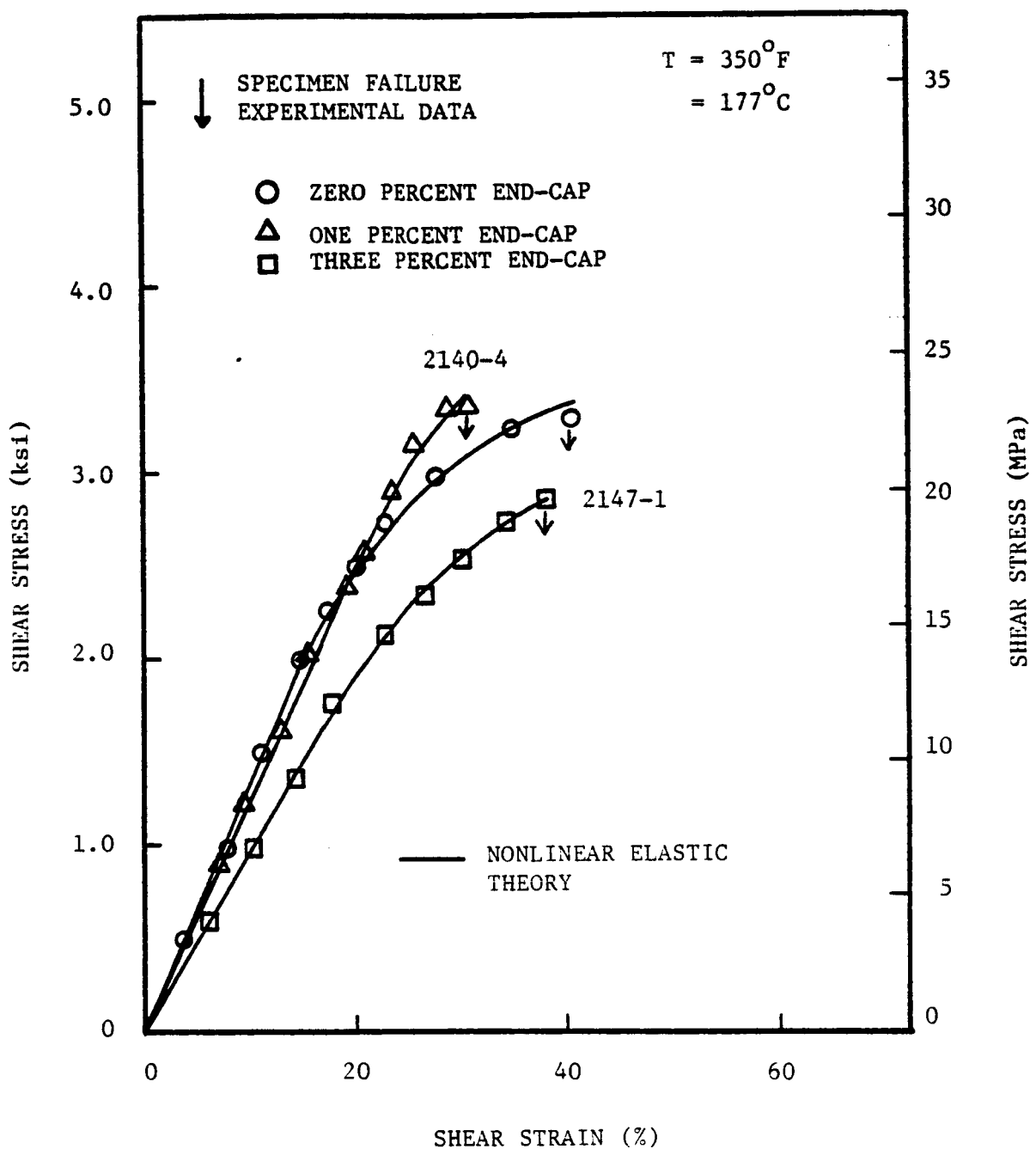


Figure 13. Constant Strain Rate Stress Strain Behavior
 of Thermoplastic Polyimidesulfone Adhesive and
 Comparison with Theory.

Table 5

Coefficients used to fit the nonlinear relation
(equations 12 and 13) to the constant strain rate stress strain behavior
of Thermoplastic Polyimidesulfone Adhesive (see figures 11, 12, and 13)

Percent End-Cap	T OF (°C)	τ_y kai (MPa)	G kai (MPa)	D kai (MPa)	n
0	70 (21)	3.0 (20.7)	18.1 (124.7)	0.010 (0.069)	2.44
1	70 (21)	2.9 (20.0)	14.3 (98.5)	0.027 (0.186)	1.89
3	70 (21)	2.3 (15.8)	7.3 (50.3)	0.073 (0.503)	1.74
0	250 (121)	2.3 (15.8)	24.2 (166.7)	0.016 (0.110)	2.16
1	250 (121)	3.0 (20.7)	20.7 (142.6)	0.015 (0.103)	2.01
3	250 (121)	2.7 (18.6)	16.5 (113.7)	0.018 (0.124)	2.18
0	350 (177)	2.0 (13.8)	13.3 (91.6)	0.031 (0.214)	2.09
1	350 (177)	2.9 (20.0)	12.2 (84.1)	0.034 (0.234)	1.80
3	350 (177)	1.9 (13.1)	9.6 (66.1)	0.062 (0.427)	1.72

Nonlinear Elastic Relation:

$$\gamma = \frac{\tau}{G}, \quad (\tau \leq \tau_y)$$

$$\gamma = D \tau^m, \quad (\tau < \tau_y)$$

°C), and 350 °F (177 °C) are shown in figures 14, 15, and 16 respectively. The adhesive's resistance to creep in the primary and secondary regions is characteristic of linear thermoplastics. Contrary to expectations, observations do not show a strong trend of increasing creep strains with increasing temperature. This may be caused by the level of molecular weight. The chain entanglement may be sufficiently low to force the strain to be more dependent upon the polymer network than temperature and secondary factors. The decrease in safe creep stress levels at 350 °F (177 °C) may be caused by decreased viscosity due to increased temperature, allowing chain slippage to occur at lower stress levels.

Figures 17, 18, and 19 show the creep results of one percent endcapped specimens at 70 °F (21 °C), 250 °F (121 °C), and 350 °F (177 °C), respectively. Creep strains increase as the temperature is increased. This is expected due to decreasing viscosity and increasing molecular motion. Decreases in the levels of safe creep stresses are also observed with increasing temperatures.

Figure 20 illustrates creep strains at comparable stress levels applied for 50 minutes for zero, one, and three percent endcapped specimens. The strains plotted are all from secondary creep regions. The creep strains decrease as molecular weight is increased. This behavior is expected since increases in molecular weight result in increasing

viscosity and decreasing chain mobility.

Figures 21, 22, and 23 show comparison of creep-rupture data with Crochet's equation based on the Maxwell (equation 25) and Chase-Goldsmith (equation 27) models for three, one, and zero percent endcapped Thermoplastic Polyimidesulfone adhesives, respectively. Apparently, in most situations, Crochet's equation based on the Chase-Goldsmith model provides a better fit to the experimental data in comparison to the solution with the Maxwell model. The Chase-Goldsmith form of the equation predicts a much faster approach to the asymptotic safe creep stress levels. The appropriate constants used in fitting Crochet's equation based on the Maxwell and Chase-Goldsmith models are shown in tables 6 and 7, respectively.

The maximum safe stress levels under creep conditions at room temperature, 250 °F (121 °C), and 350 °F (177 °C) are shown in figure 24. At room temperature there is an increase of approximately 17% as the molecular weight increases by 7.4 %. The safe creep stress level remains relatively constant when the molecular weight is increased by another 4.6 %. The increase is expected due to the increasing chain entanglement and increasing degree of intermolecular forces. The nearly constant values of maximum ultimate shear stress, between one and zero percent endcapping, on the other hand, may be caused by decreasing adhesion as the viscosity increases with molecular weight

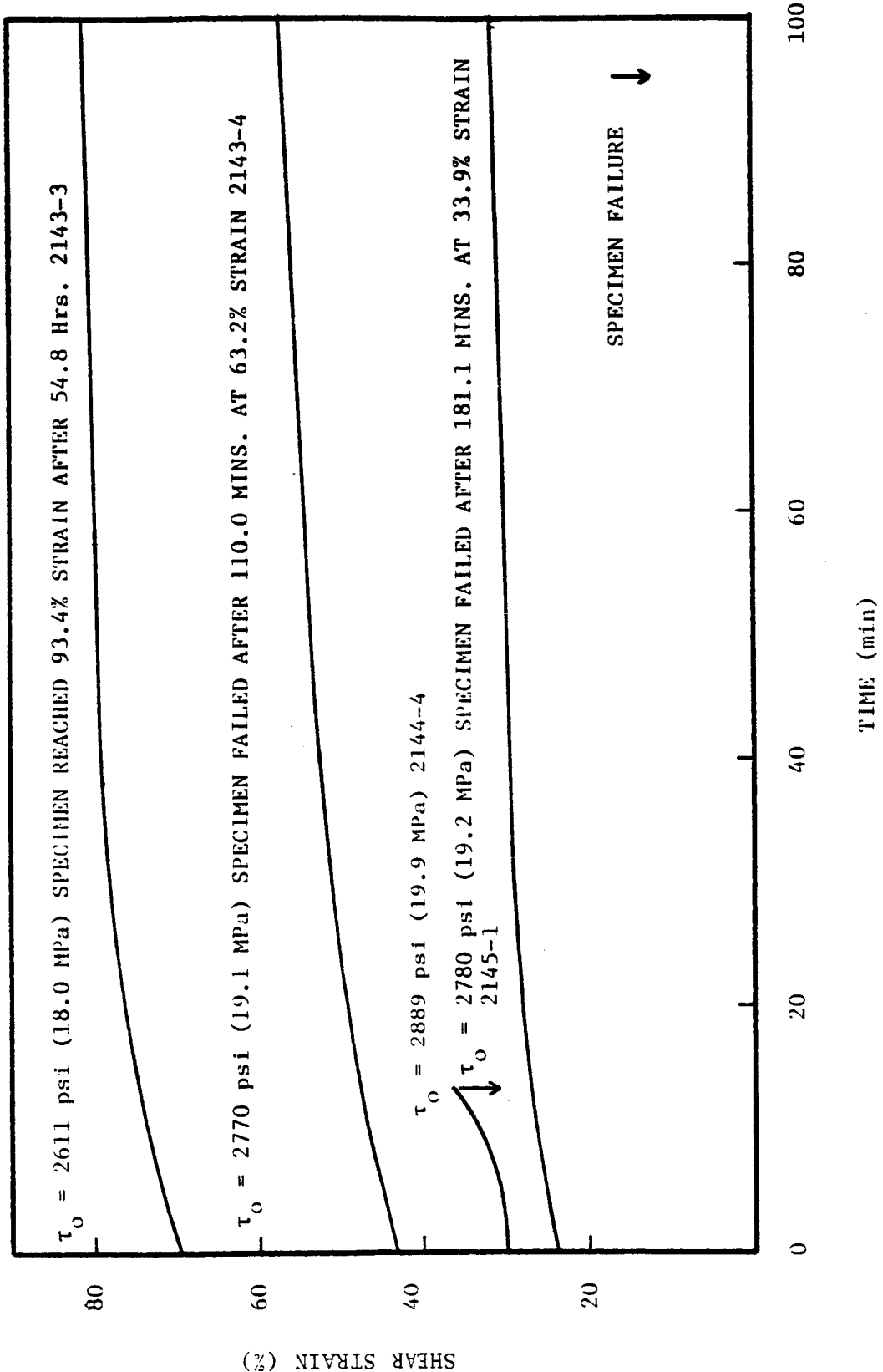


Figure 14. Creep Behavior of Three Percent End-Cap Thermoplastic Polyimidesulfone Adhesive at 70°F (21°C) Condition.

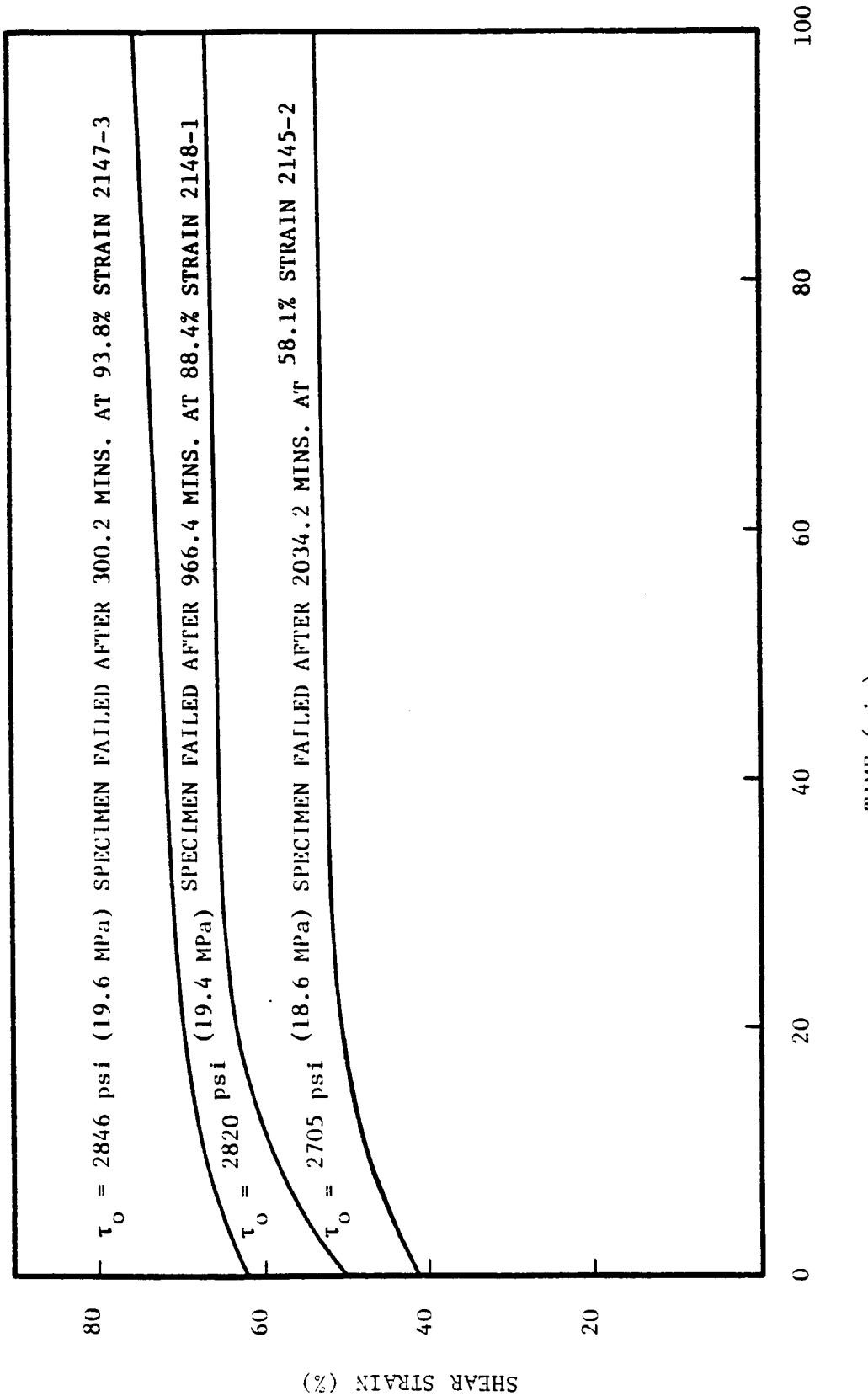


Figure 15. Creep Behavior of Three Percent End-Cap Thermoplastic Polyimidesulfone Adhesive at 250°F (121°C) Condition.

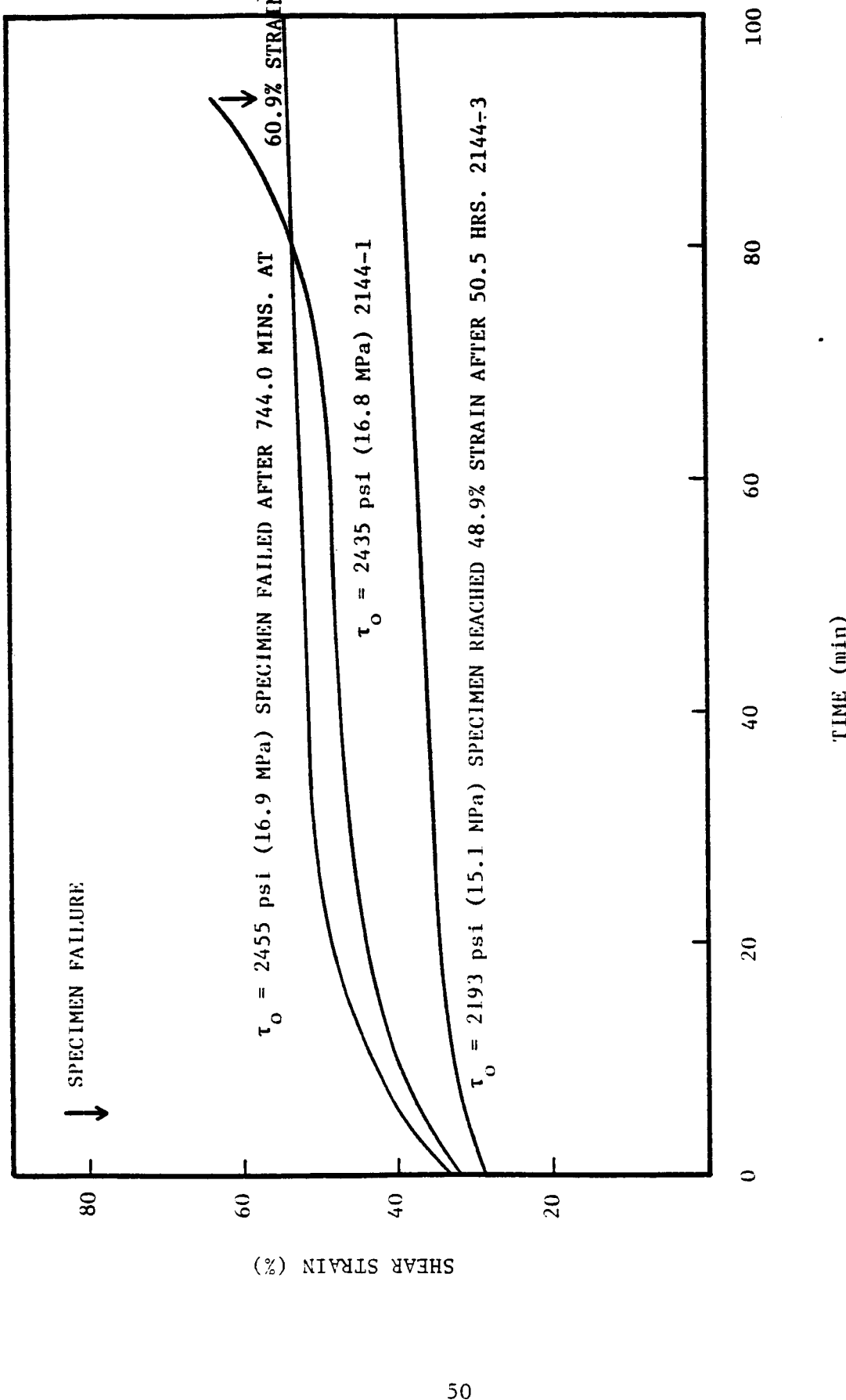


Figure 16. Creep Behavior of Three Percent End-Cap Thermoplastic Polyimidesulfone Adhesive at 350°F (177°C) Condition.

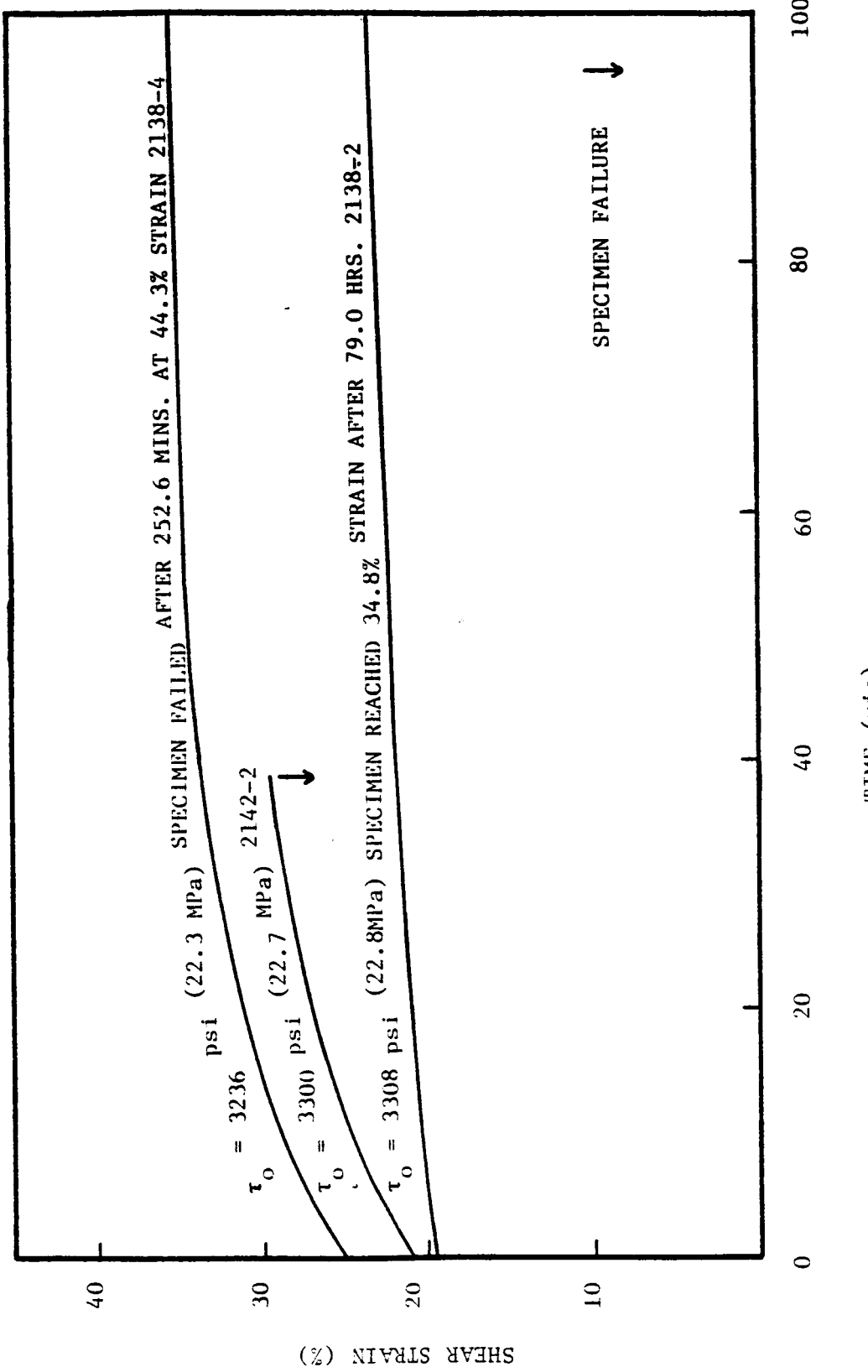


Figure 17. Creep Behavior of One Percent End-Cap Thermoplastic Polyimidesulfone Adhesive at 70°F (21°C) Condition.

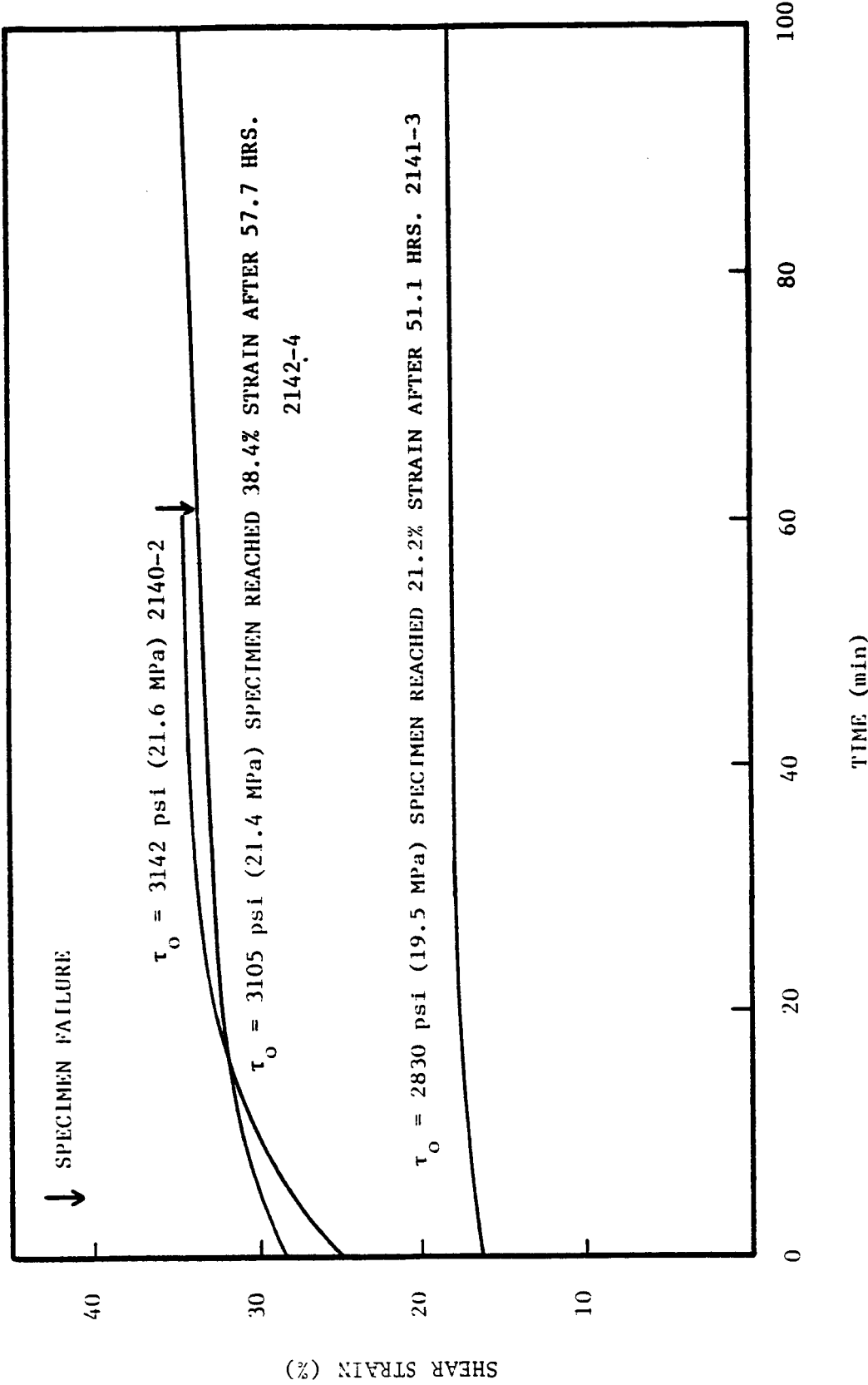


Figure 18. Creep Behavior of One Percent End-Cap Thermoplastic Polyimidesulfone Adhesive at 250°F (121°C) Condition.

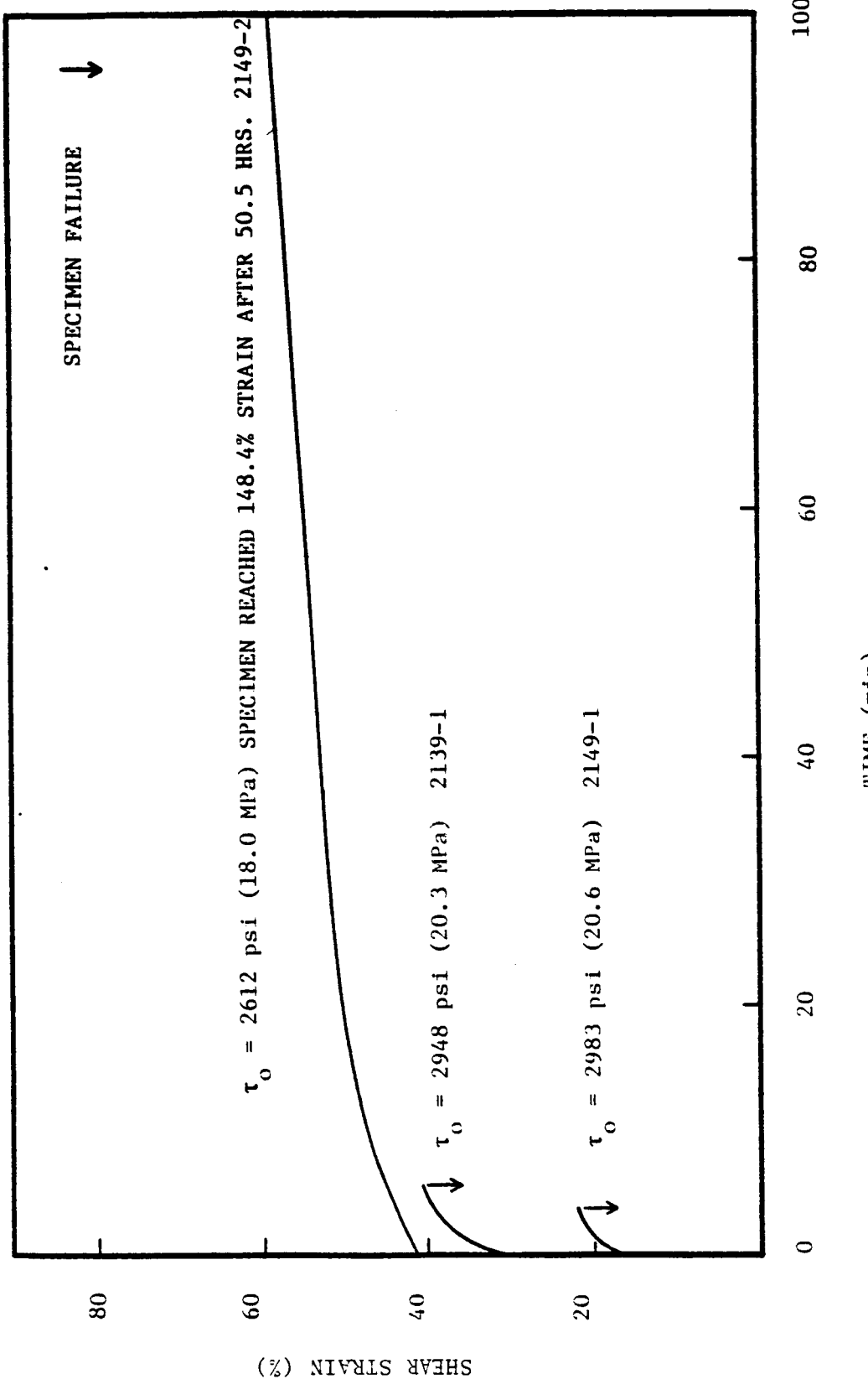


Figure 19. Creep Behavior of One Percent End-Cap Thermoplastic Polyimidesulfone Adhesive at 350°F (177°C) Condition.

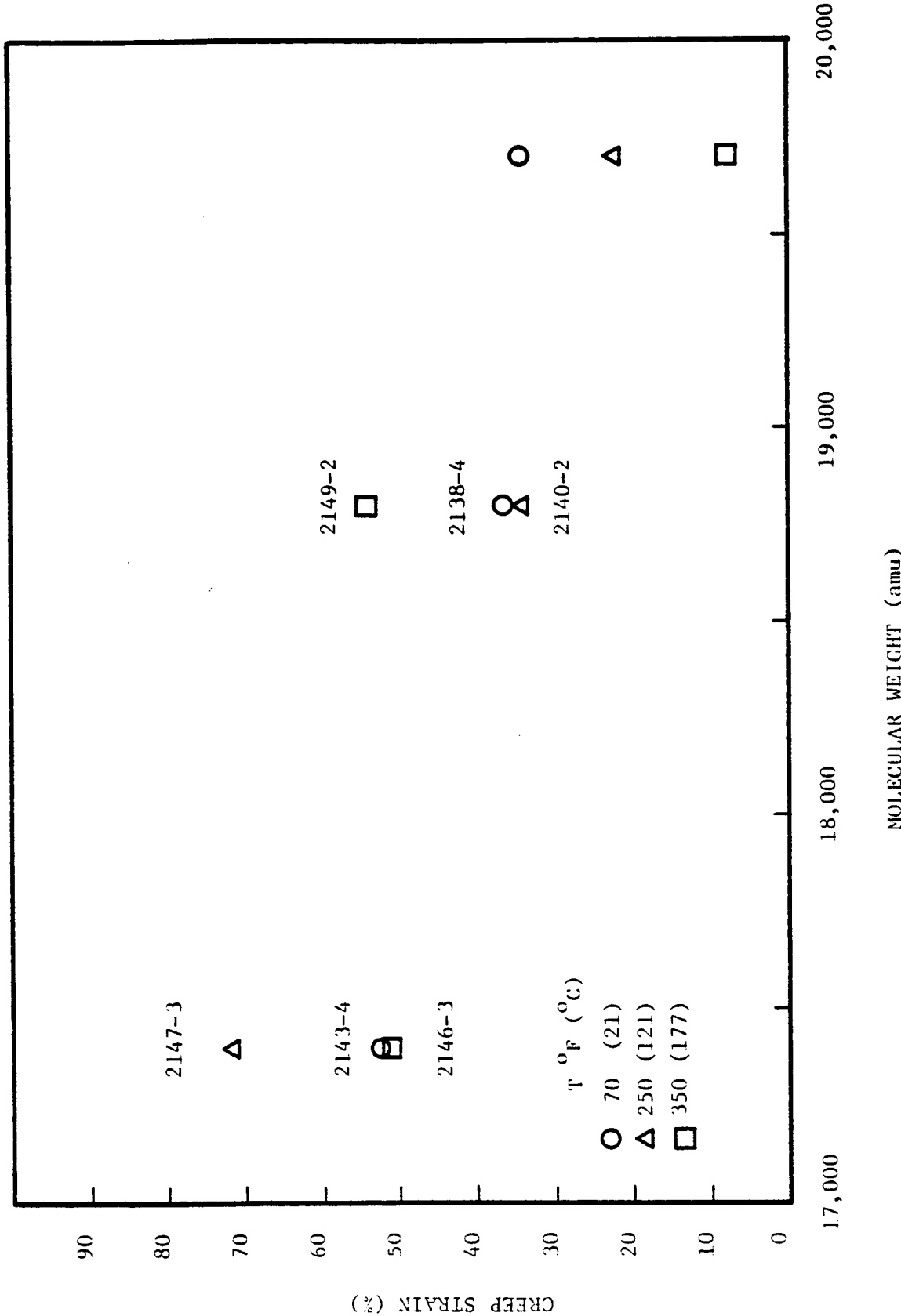


Figure 20. Variation of Creep Strains at 50 Minutes with Molecular Weight for Thermoplastic Polyimidesulfone Adhesive.

Table 6

Constants used in fitting Crochet's equation based on the
Maxwell model for zero, one, and three percent endcapped
Thermoplastic Polyimidesulfone adhesive
(see figures 21, 22, and 23)

Percent End-Cap	Temp °F (°C)	A psi (MPa)	B psi (MPa)	C psi-min (MPa-min)
0	70 (21)	3267 (22.5)	1054 (7.3)	46.7×10^{-6} (0.32x10 ⁻⁶)
1	70 (21)	3239 (22.3)	579 (4.0)	7.3×10^{-6} (0.05x10 ⁻⁶)
3	70 (21)	2769 (19.1)	467 (3.2)	10.8×10^{-6} (0.07x10 ⁻⁶)
0	250 (121)	2765 (19.0)	685 (4.7)	27.4×10^{-6} (0.19x10 ⁻⁶)
0	350 (177)	2270 (15.6)	1069 (7.4)	157.7×10^{-6} (1.09x10 ⁻⁶)
1	350 (177)	2889 (19.9)	477 (3.3)	126.7×10^{-6} (0.87x10 ⁻⁶)
3	350 (177)	2434 (16.8)	430 (3.0)	25.8×10^{-6} (0.18x10 ⁻⁶)

Crochet's Equation Based on the Maxwell Model:

$$\tau = A + B \exp[-C\tau \frac{t}{\eta}]$$

Table 7

Constants used in fitting Crochet's equation based on the Chase-Goldsmith model for zero, one, and three percent encapped Thermoplastic Polyimidesulfone adhesive (see figures 21, 22 and 23)

Percent End-Cap	T °F (°C)	A psi (MPa)	B psi (MPa)	C psi (MPa)	G ₁ ksi (MPa)	G _∞ ksi (MPa)	τY ksi-sec (MPa)	n
0	70 (21)	3267 (22.5)	1054 (7.3)	115.7 (0.80)	25.1 (172.9)	4.4 (30.3)	3.8 (26.2)	3.0 (20.7)
1	70 (21)	3239 (22.3)	579 (4.0)	13.9 (0.10)	30.5 (210.1)	1.0 (6.9)	1.0 (6.9)	2.7 (18.6)
3	70 (21)	2769 (19.1)	467 (3.2)	4.2 (0.03)	3.4 (23.4)	0.5 (3.4)	0.4 (2.8)	2.1 (14.5)
0	250 (121)	2765 (19.0)	685 (4.7)	27.2 (0.19)	24.2 (166.7)	2.1 (14.5)	2.0 (13.8)	2.3 (15.8)
0	350 (177)	2270 (15.6)	1069 (7.4)	25.8 (0.18)	13.3 (91.6)	1.0 (6.9)	0.9 (6.2)	2.0 (13.8)
1	350 (177)	2889 (19.9)	477 (3.3)	21.2 (0.15)	12.2 (84.1)	1.7 (11.7)	1.5 (10.3)	2.7 (18.6)
3	350 (177)	2434 (16.8)	430 (3.0)	15.8 (0.11)	9.6 (66.1)	1.3 (9.0)	1.1 (7.6)	1.9 (13.1)
								2.9 (20.0)

$$\begin{aligned}
 \text{Crochet's Equation Based on the Chase-Goldsmith Model:} \quad Y(t) = & A + B \exp \left\{ -C \left[\frac{\tau Y}{G_1} \left(\exp \left[-\frac{G_1}{n} t \right] - 1 \right) \right. \right. \\
 & + \frac{Y(t)}{G_\infty} \left(1 - \exp \left[-\frac{G_1}{n} t \right] \right) \\
 & \left. \left. + \frac{Y(t)}{G_\infty} \left(\exp \left[-\frac{G_1}{n} t \right] - 1 \right) \right\}
 \end{aligned}$$

beyond a point where optimum interfacial bond formation is no longer possible. The safe creep stress levels are also observed to increase with molecular weight at higher temperatures for the one and three percent endcapped specimens. The significant decreases in the safe creep stress levels at zero percent endcap value under elevated temperatures is attributed to the high temperature interfacial failures as discussed previously.

Figure 25 illustrates the variation of safe creep stress with temperature for zero, one, and three percent endcapped Thermoplastic Polyimidesulfone adhesive. Increasing safe creep stress levels are observed with increased molecular weight (excluding the zero percent end-cap values at elevated temperatures). The safe creep stress versus temperature behavior of the one and three percent endcapped specimens is very similar. This suggests that the degree of decrease in viscosity and increase in chain mobility with increasing temperature is relatively constant for the molecular weight values examined.

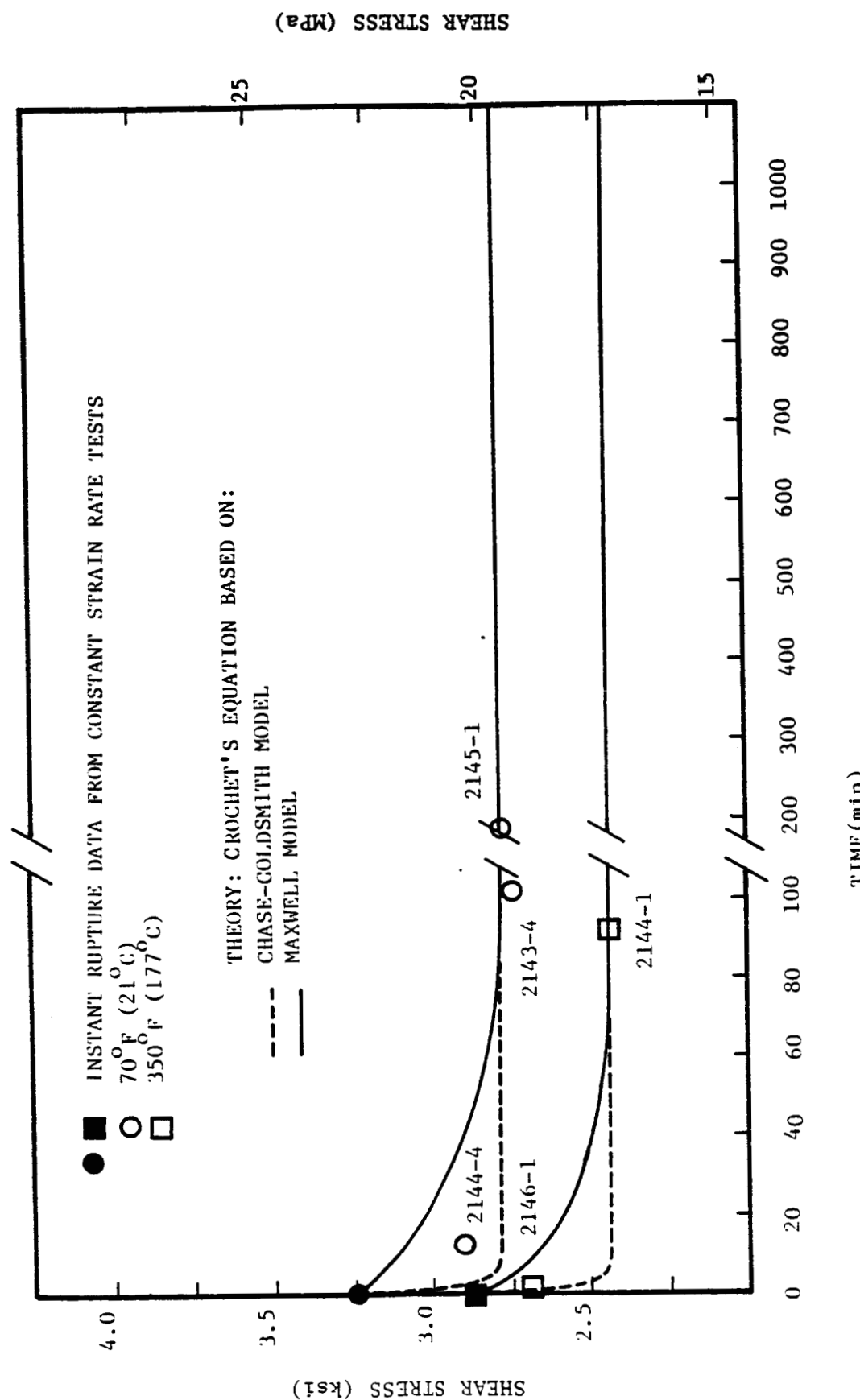


Figure 21. Creep Rupture Data and Comparison with Theory for Three Percent End-Cap Thermoplastic Polyimidesulfone Adhesive.

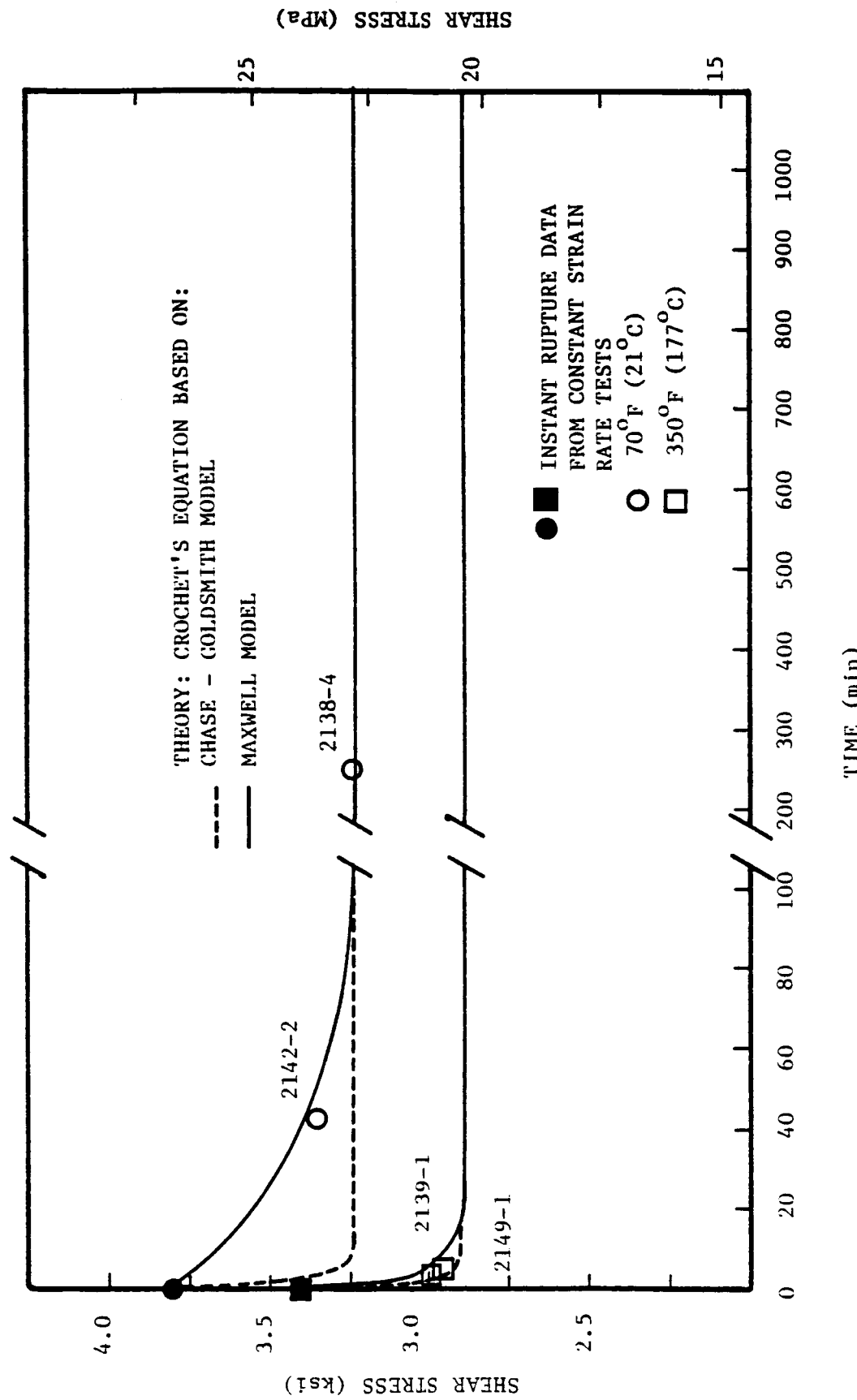


Figure 22. Creep Rupture Date and Comparison with Theory for One Percent End-Cap Thermoplastic Polyimidesulfone Adhesive.

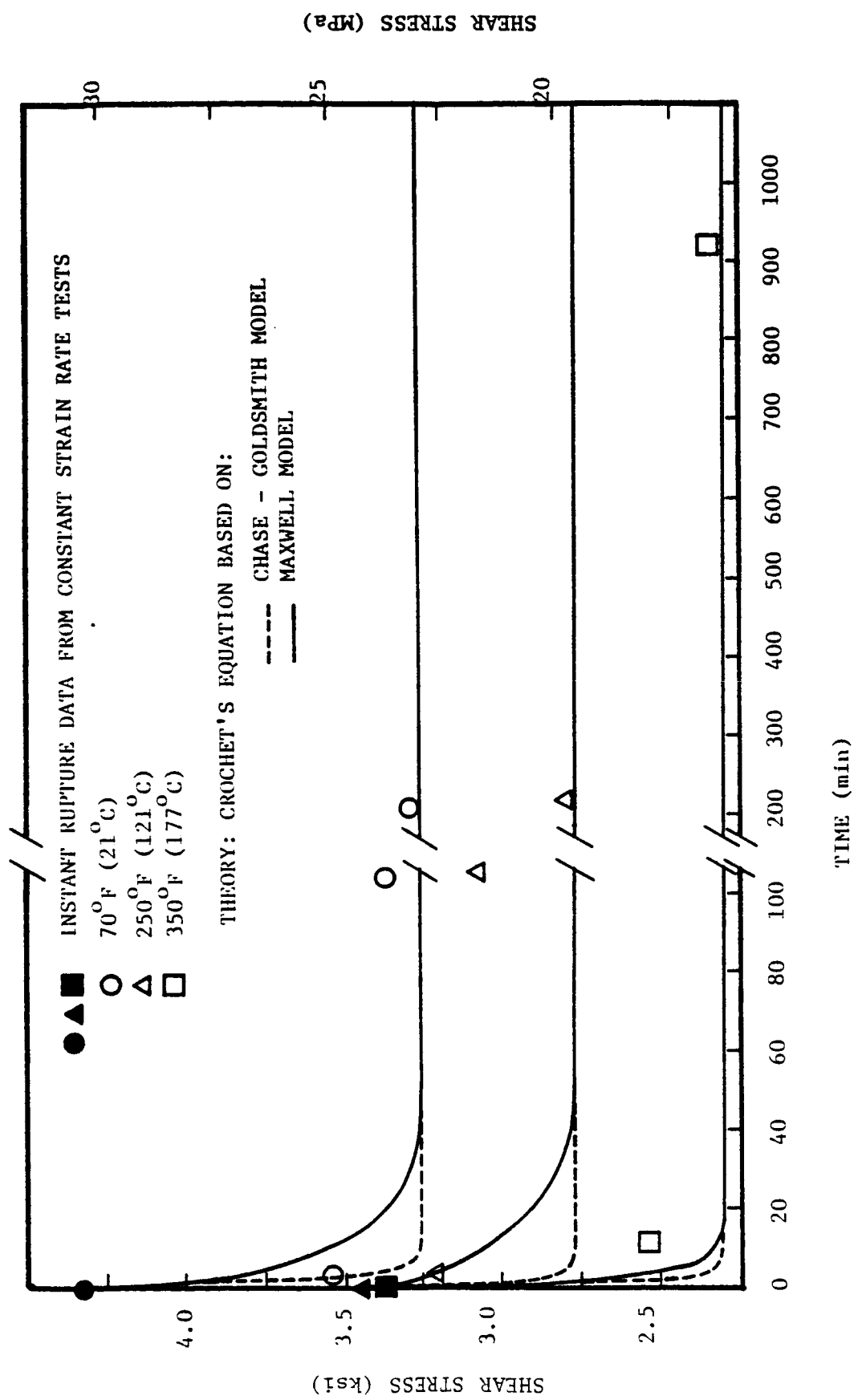


Figure 23. Creep Rupture Data and Comparison with Theory for Zero Percent End-Cap Thermoplastic Polyimidesulfone Adhesive.

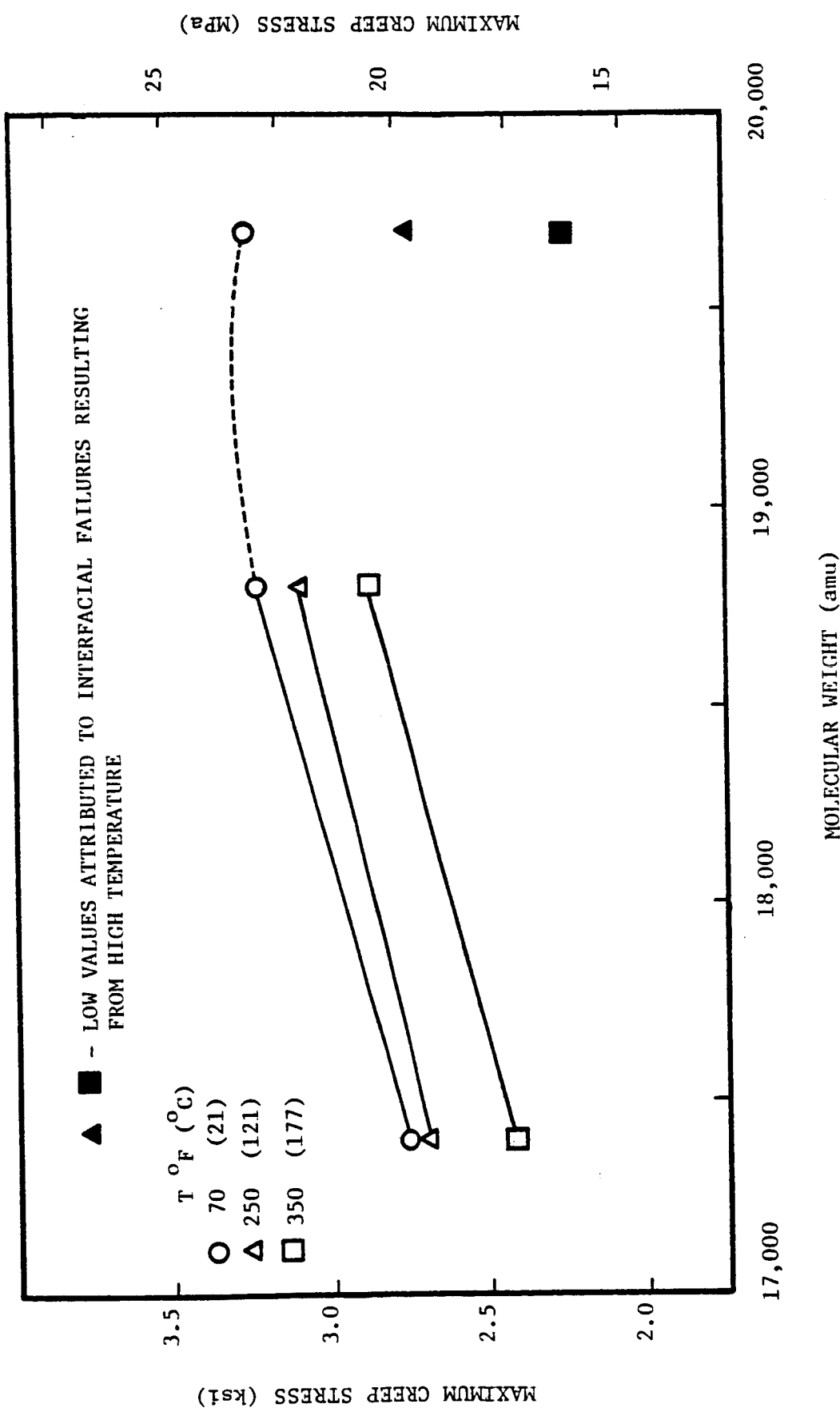


Figure 24. Variation of Maximum (Safe) Creep Stress with Molecular Weight for Thermoplastic Polyimidesulfone Adhesive.

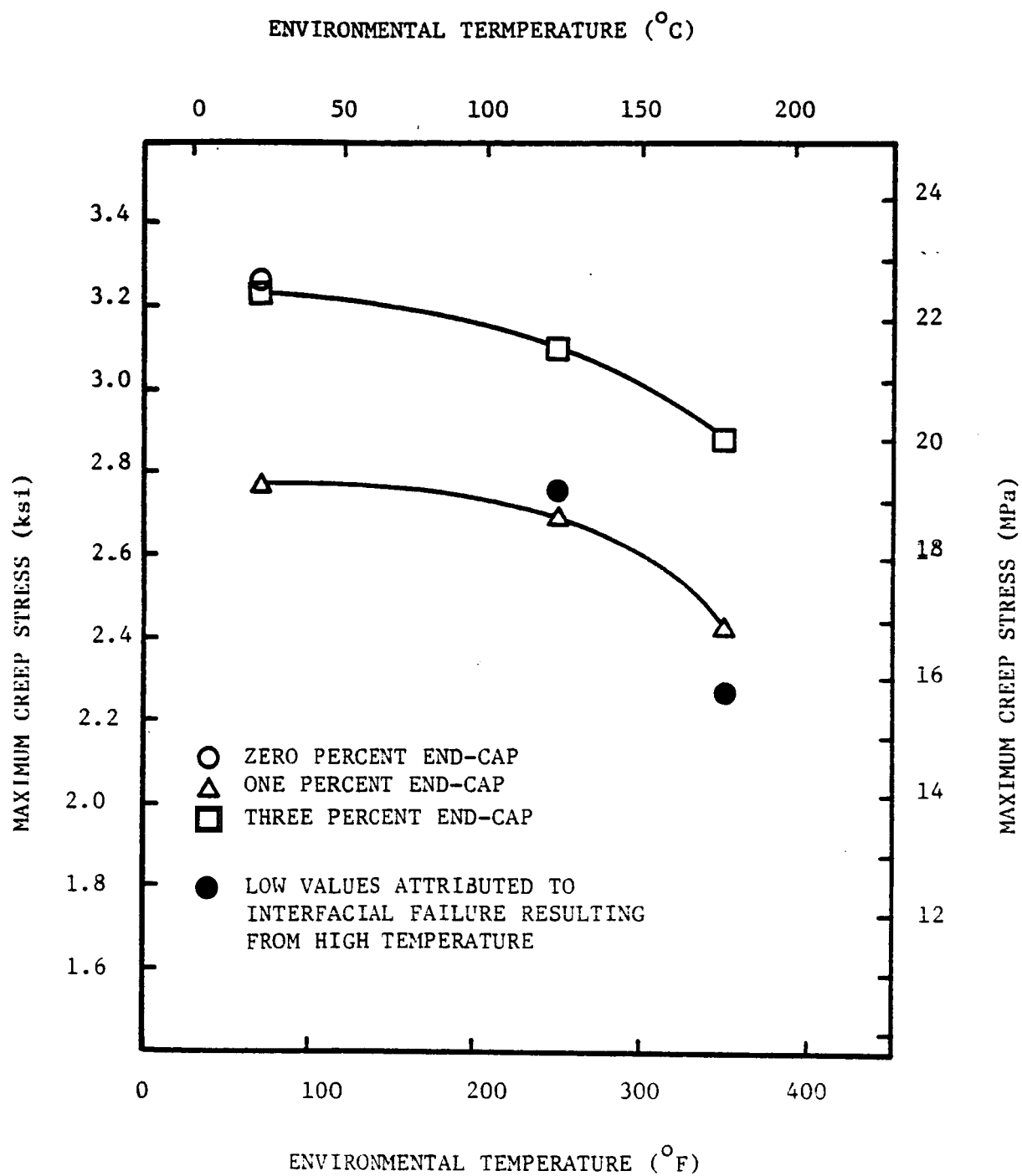


Figure 25. Variation of Maximum (Safe) Creep Stress with Environmental Temperature for Different End-Cap Forms of Thermoplastic Polyimidesulfone Adhesive.

CHAPTER 5

CONCLUSIONS

The effects of molecular weight on the shear creep and constant strain rate behavior of Thermoplastic Polyimidesulfone adhesive was studied in the bonded form. For this purpose, constant strain rate, creep, and creep-rupture experiments were performed on zero [14], one, and three percent endcapped specimens of the adhesive.

Mathematical relations were proposed to represent the constant strain rate and delayed failure viscoelastic-plastic behavior of Thermoplastic Polyimidesulfone adhesive. Based on the mathematical relations, used in conjunction with experimental results, several conclusions can be derived:

It is possible to describe the constant strain rate shear stress strain behavior of zero, one, and three percent endcapped Thermoplastic Polyimidesulfone adhesive using viscoelastic Chase-Goldsmith model or nonlinear elastic relations;

Ludwik's equation does not reveal changing rate dependence (pertaining to ultimate shear stresses and strains) with changing molecular weights;

Crochet's equation based on the Chase-Goldsmith model provides a better description of the delayed failure data in comparison to Crochet's equation based on the Maxwell model;

Room temperature constant strain rate results show increases in viscosity with increasing molecular weight (it should be noted, however, that these viscosity coefficient values are calculated parameters obtained on the basis of the Chase-Goldsmith model and they do not represent values measured using standard viscosity measurement techniques);

Nonlinear relations reveal increasing strain-hardening capacity with increasing molecular weight;

At all temperature levels of experimentation, ultimate shear stress levels and safe creep stress levels increased with increasing molecular weight.

Reductions in molecular weight revealed increased adhesion (less interfacial failure), but also reduced the cohesive strength of the model adhesive. In general, the results of this investigation imply that reductions in the molecular weight of Thermoplastic Polyimidesulfone adversely affect the mechanical properties studied. Reductions in molecular weight may increase wetting and diffusion during the bonding process, but these effects are insufficient to override the advantages of increased intermolecular and intramolecular forces created at higher molecular weights.

REFERENCES

1. St. Clair, T.L. and Yamaki, D.A., "A Thermoplastic Polyimidesulfone," NASA Langley Research Center, Technical Memorandum No. 84574, Nov. 1982.
2. Singh, J.J., St. Clair, T.L. and Walker, S., "A Study of the Effects of End-Cap Molecular Species on Environmental Characteristics of Polyimidesulfones," NASA Langley Research Center, Technical Memorandum No. 86283, Aug. 1984.
3. Siggia, S. and Mark, H. F. , Polymer Science and Materials, Ed. Tobolsky, A.V. and Mark, H.F., John Wiley and Sons, Inc., New York (1971), pp 56-57.
4. Alfrey, T. Jr., Mechanical Behavior of High Polymers, Interscience Publishers, Inc., New York (1948), pp. 493-498.
5. Tsuji, T., Masuoka, M. and Nakao, K., "Superposition of Peel Rate, Temperature and Molecular Weight for T Peel Strength of Polyisobutylene," Adhesion and Adsorption of Polymers, Plenum Publishing Corp., 1980.
6. Zhurkov, S. N., "Kinetic Concept of the Strength of Solids," Internl. J. of Frac. Mech., 1 (4), 331-323 (1965).
7. Mark, H. F., Polymer Science and Materials, Ed. Tobolsky, A.V. and Mark, H.F., John Wiley and Sons, Inc., New York (1971), p 236.
8. Margolies, A. F. , "Effect of Molecular Weight on Properties of HDPE," Soc. Plas. Eng. J., 27, 44, June 1971.
9. Fellers, J. F. and Kee, B. F. , "Crazing Studies of Polystyrene. I. A New Phenomenological Observation," Journal of Applied Polymer Science, John Wiley and Sons, Inc., 18, pp 2355-2365, (1964).
10. Knauss, W.G., "The Mechanics of Polymer Fracture," App. Mechanics Reviews, Jan. 1973.
11. Gardner, R. J. and Martin, J. R., "Humid Aging of Plastics: Effects of Molecular Weight on Mechanical Properties and Fracture Morphology of Polycarbonate," J. of App. P. Sci., 24, 1269-1280, 1979.
12. Vlachopoulos, J., Hadjis, N., and Hamielec, A. E., "Influence of Molecular Weight on the Tensile Properties of Nearly Monodisperse Polystyrenes,"

Polymer, 19, 115, 1977.

13. Shinozaki, D. M. , Woo, K. , Vlachopoulos, J. and Hamielec, A., "Influence of Processing Parameters and Molecular Weight on the Mechanical Properties of PVC," J. App. P. Sci., 21, 3345-3354, 1977.
14. Schenck , S. C. and Sancaktar , E. , " Material Characterization of Structural Adhesives in the Lap Shear Mode," NASA Langley Research Center, NASA Contractor Report No. 172237, Sept. 1983.
15. Sancaktar, E. and Padgilwar, S., " The Rate and Time Dependent Material Characterization of LARC-3 Structural Adhesive," Clarkson College, Potsdam, New York, Report No. MIE-069, April 1981.
16. Nielsen, L. E. , Mechanical Properties of Polymers, Reinhold Publishing Corp., New York (1962),pp. 56-57.
17. Fox, T.G. and Flory, P.J., "Further Studies on the Melt Viscosity of Polyisobutylene," The Journal of Physical and Colloid Chemistry, Ed. Lind, S.C., 55, 221-234, 1951.
18. Wu, S. , Polymer Interface and Adhesion, Marcel Dekker, Inc., New York (1982), p. 403.
19. Renieri, M. P., Herakovich, C. T. and Brinson, H. F., "Rate and Time Dependent Behavior of Structural Adhesives," Virginia Polytechnic Institute, Report No. VPI-E-76-7, April 1976.
20. Sancaktar, E. and Schenck, S.C., "Temperature Dependent Creep Rupture of Structural Adhesives," Proceedings of the Southeastern XIIth Conference on Theoretical and Applied Mechanics, Vol. 2, 148-153 (1984).
21. Brinson, H. F., Renieri, M. P. and Herakovich, C. T., " Rate and Time Dependent Failure of Structural Adhesives," Fracture Mechanics of Composites, ASTM STP 593, 1975,pp. 177-199.
22. Brinson, H. F. , Deformation and Fracture of High Polymers, (H.H. Kaush et al. eds.) Plenum Press, New York (1974).
23. Sancaktar, E. and Padgilwar, S., " The Effects of Inherent Flaws on the Time and Rate Dependent Failure of Adhesively Bonded Joints," Transactions of the ASME Journal of Mechanical Design, Vol. 104, 643-650, July 1982.

APPENDIX A
TABLES OF SINGLE LAP SPECIMEN DIMENSIONS

Table A-1

Dimensions for Single Lap Specimens Bonded with
One Percent Endcapped Thermoplastic Polyimidesulfone

Specimen No.	Bondline Thickness Inches (CM)	Overlap Length Inches (CM)	Overlap Width Inches (CM)
2138-2	0.00695 (0.01765)	0.52705 (1.33871)	0.98767 (2.50868)
2138-3	0.00644 (0.01636)	0.52500 (1.33350)	0.98170 (2.49352)
2138-4	0.00764 (0.01941)	0.51920 (1.31877)	0.98213 (2.49461)
2139-1	0.00731 (0.01857)	0.54515 (1.38468)	0.99560 (2.52882)
2139-3	0.00744 (0.01890)	0.53305 (1.35395)	0.98827 (2.51021)
2139-4	0.00908 (0.02306)	0.52490 (1.33325)	0.99707 (2.53256)
2140-1	0.00699 (0.01775)	0.51805 (1.31585)	0.99413 (2.52509)
2140-2	0.00610 (0.01549)	0.52900 (1.34366)	0.99287 (2.52189)
2140-4	0.00849 (0.02156)	0.53995 (1.37147)	0.99877 (2.53688)
2141-1	0.00976 (0.02479)	0.52485 (1.33312)	0.99982 (2.53954)
2141-2	0.00813 (0.02065)	0.52660 (1.33756)	0.99140 (2.51816)
2141-3	0.00819 (0.02080)	0.52455 (1.33236)	0.99350 (2.52349)
2142-1	0.00759 (0.02019)	0.53445 (1.35750)	0.99633 (2.53068)
2142-2	0.00746 (0.01895)	0.53100 (1.34874)	0.98545 (2.50304)
2142-3	0.00615 (0.01562)	0.52745 (1.33972)	0.98600 (2.50444)
2142-4	0.00674 (0.01712)	0.52080 (1.32283)	0.98930 (2.51282)
2149-1	0.00653 (0.01659)	0.52411 (1.33124)	0.99143 (2.51823)
2149-2	0.00468 (0.01189)	0.52170 (1.32512)	0.99077 (2.51656)
2149-3	0.00547 (0.01389)	0.51945 (1.31940)	0.98466 (2.50105)
2149-4	0.00673 (0.01709)	0.51661 (1.31219)	0.99993 (2.53982)

Table A-2

**Dimensions for Single Lap Specimens Bonded with
Three Percent Endcapped Thermoplastic Polyimidesulfone**

Specimen No.	Bondline Thickness Inches (CM)	Overlap Length Inches (CM)	Overlap Width Inches (CM)
2143-2	0.00321 (0.00815)	0.54105 (1.37427)	0.98950 (2.51333)
2143-3	0.00263 (0.00668)	0.54420 (1.38227)	0.98717 (2.50741)
2143-4	0.00452 (0.01148)	0.54605 (1.38697)	0.98906 (2.51221)
2144-1	0.00444 (0.01128)	0.51605 (1.31077)	0.99463 (2.52636)
2144-3	0.00352 (0.00894)	0.52860 (1.34264)	0.99184 (2.51927)
2144-4	0.00495 (0.01257)	0.53295 (1.35369)	0.99297 (2.52214)
2145-1	0.00450 (0.01143)	0.52405 (1.33109)	0.99660 (2.53136)
2145-2	0.00399 (0.01013)	0.52174 (1.32522)	0.99213 (2.52001)
2145-4	0.00435 (0.01105)	0.52313 (1.32875)	0.99210 (2.51993)
2146-1	0.00313 (0.00795)	0.49911 (1.26774)	0.96990 (2.46355)
2146-2	0.00322 (0.00818)	0.51815 (1.31610)	0.97176 (2.46827)
2146-3	0.00318 (0.00808)	0.53435 (1.35725)	0.96817 (2.45915)
2147-1	0.00317 (0.00805)	0.51960 (1.31978)	0.99120 (2.51765)
2147-2	0.00316 (0.00803)	0.52600 (1.33604)	0.98587 (2.50411)
2147-3	0.00309 (0.00785)	0.53150 (1.35001)	0.99157 (2.51859)
2147-4	0.00369 (0.00937)	0.53541 (1.35994)	0.99501 (2.52733)
2148-1	0.00308 (0.00782)	0.51842 (1.31679)	0.99198 (2.51963)
2148-2	0.00472 (0.01199)	0.51973 (1.32011)	0.99372 (2.52405)
2148-3	0.00547 (0.01389)	0.51942 (1.31933)	0.98461 (2.50091)
2148-4	0.00593 (0.01506)	0.52601 (1.33607)	0.99104 (2.51724)